Ángel Rodríguez Ballabriga

Analysis of amplitude integrated electroencephalography in neonates: Assessing performance of aCUP-E versus liquid gel electrodes

Final degree project

Directed by Dr. Albert Fabregat Sanjuan

Directed by Dr. Vicenç Pascual Rubio

Bachelor's Degree in Biomedical Engineering

UNIVERSITAT ROVIRA I VIRGILI

Tarragona

2023

Acknowledgements

First, I would like to thank Dr. Albert Fabregat Sanjuan and Dr. Vicenç Pascual Rubio, for their commitment during the work. The help in the triage and approach of the subject, as well as the weekly follow-up meetings, have been key factors for the development of the work.

Thank the personnel of the Clinical Neurophysiology Department of the *Hospital Sant Joan de Reus* for their collaboration on the clinical research and for making this study possible.

I would also like to express my heartfelt gratitude to my parents and brother. Their encouragement and belief in me have been invaluable throughout this journey. I am very grateful for their continuous support and inspiration. Their guidance and sacrifices have been the foundation of my success, being my unwavering pillars of strength.

Finally, I would like to thank everyone that at some point has encouraged me and helped me through the process. Also, to *Universitat Rovira I Virgili,* who has provided me with an exceptional academic environment and resources, which have made me grow both academically and personally.

It has been four years that I will never forget, thank you all.

Abstract

Neonatal Intensive Care Units (NICUs) face significant challenges when addressing neurological emergencies and ensuring optimal neurocritical care for newborns. While advancements in neonatal monitoring have improved the survival rates of infants, the evaluation of brain function with amplitude integrated electroencephalography (aEEG) remains an area requiring further development.

Neonatologists and clinical neurophysiologists agree that there are no adequate electrodes that allow long-lasting recordings. As a result, aEEG loses power to diagnose cerebral damage as Hypoxic-Ischemic Encephalopathy (HIE) or epilepsy in NICUs.

In this work, a comparative analysis between commercial liquid-gel electrodes and a new and specific electrode (aCUP-E) is executed to evaluate their performance in a clinical trial with 15 neurologically healthy neonates, 4 at term and 11 preterm. The definition of certain neurophysiology criteria has made it possible to achieve the goal of determining optimal and non-optimal brain activity. Impedance and signal characteristics have also been computed, together with a survey among the NICU personnel.

The results show that aCUP-E records larger optimal activity thanks to its adaption and fixation to the scalp of the neonate together with the ability to refill with electroconductive gel. These improvements enhance the stability of the impedance and the quality of the recordings. Moreover, the survey has shown a clear willingness of the NICUs personnel to use the new electrode. As a conclusion, this research highlights the limitations of current electrodes in aEEG and states that aCUP-E could be a better alternative.

Keywords: aEEG, HIE, neurophysiology, liquid-gel electrodes, aCUP-E, impedance.

Resumen

Las Unidades de Cuidados Intensivos Neonatales (UCIN) se enfrentan a importantes retos a la hora de abordar las urgencias neurológicas y garantizar unos cuidados neurocríticos óptimos a los recién nacidos. Aunque los avances en la monitorización neonatal han mejorado las tasas de supervivencia de los recién nacidos, la evaluación de la función cerebral con electroencefalografía de amplitud integrada (aEEG) sigue siendo un área que requiere un mayor desarrollo.

Los neonatólogos y los neurofisiólogos clínicos coinciden en que no existen electrodos adecuados que permitan realizar registros de larga duración. Como consecuencia, la aEEG pierde potencia para diagnosticar daños cerebrales como la encefalopatía hipóxico-isquémica (EHI) o la epilepsia en las UCIN.

En este trabajo se realiza un análisis comparativo entre electrodos comerciales de gel líquido y un electrodo nuevo y específico (aCUP-E) para evaluar su rendimiento en un ensayo clínico con 15 neonatos neurológicamente sanos, 4 a término y 11 prematuros. La definición de determinados criterios neurofisiológicos ha permitido alcanzar el objetivo de determinar la actividad cerebral óptima y no óptima. También se han calculado características tanto de la impedancia como de la señal, y se ha realizado una encuesta entre el personal de la UCIN.

Los resultados muestran que aCUP-E registra una actividad óptima mayor gracias a su adaptación y fijación al cuero cabelludo del neonato junto con la capacidad de recambiar el gel electroconductor. Estas mejoras aumentan la estabilidad de la impedancia y la calidad de los registros. Además, la encuesta ha mostrado una clara disposición del personal de las UCIN a utilizar el nuevo electrodo. Como conclusión, esta investigación pone de manifiesto las limitaciones de los electrodos actuales en aEEG y afirma que aCUP-E podría ser una alternativa mejor.

Palabras clave: aEEG, EHI, neurofisiología, electrodos de gel líquido, aCUP-E, impedancia.

Resum

Les Unitats de Cures Intensives Neonatals (UCIN) s'enfronten a reptes importants a l'hora d'abordar les urgències neurològiques i garantir unes cures neurocrítiques òptimes als nadons. Tot i que els avenços en el monitoratge neonatal han millorat les taxes de supervivència dels nounats, l'avaluació de la funció cerebral amb electroencefalografia d'amplitud integrada (aEEG) continua sent una àrea que requereix un desenvolupament més gran.

Els neonatòlegs i els neurofisiòlegs clínics coincideixen que no hi ha elèctrodes adequats que permetin realitzar registres de llarga durada. Com a conseqüència, l'aEEG perd potència per diagnosticar danys cerebrals com l'encefalopatia hipòxico-isquèmica (EHI) o l'epilèpsia a les UCIN.

En aquest treball es realitza una anàlisi comparativa entre elèctrodes comercials de gel líquid i un elèctrode nou i específic (aCUP-E) per avaluar-ne el rendiment en un assaig clínic amb 15 nounats neurològicament sans, 4 a terme i 11 prematurs. La definició de determinats criteris neurofisiològics ha permès assolir l'objectiu de determinar l'activitat cerebral òptima i no òptima. També s'han calculat característiques tant de la impedància com del senyal i s'ha fet una enquesta entre el personal de la UCIN.

Els resultats mostren que aCUP-E registra una activitat òptima més gran gràcies a la seva adaptació i fixació al cuir cabellut del nounat juntament amb la capacitat de recanviar el gel electroconductor. Aquestes millores augmenten l'estabilitat de la impedància i la qualitat dels registres. A més, l'enquesta ha mostrat una clara disposició del personal de les UCIN a fer servir el nou elèctrode. Com a conclusió, aquesta investigació posa de manifest les limitacions dels elèctrodes actuals a aEEG i afirma que aCUP-E podria ser una alternativa millor.

Paraules clau: aEEG, EHI, neurofisiologia, elèctrodes de gel líquid, aCUP-E, impedància.

Abbreviations and acronyms

aCUP-E: Advanced Cup Electrode

NICU: Neonatal Intensive Care Unit

EEG: Electroencephalography

aEEG: Amplitude Integrated Electroencephalography

vEEG: video Electroencephalography

CFM: Cerebral Function Monitor

ECG: Electrocardiogram

MRI: Magnetic Resonance Imaging

HIE: Hypoxic-Ischemic Encephalopathy

NS: Neonatal Seizure

TH: Therapeutic Hypothermia

SDA: Seizure Detection Algorithm

DOR: Diagnostic Odds Ratio

CMRR: Common Mode Rejection Ratio

FIR: Finite Impulse response

EMI: Electromagnetic Interference

SNR: Signal to Noise Ratio

RMSD: Root Mean Square Deviation

RMSE: Root Mean Square Error

ICA: Independent Component Analysis

SD: Standard Deviation

FFT: Fast Fourier Transform

UI: User Interface

HUSJR: Hospital Universitari Sant Joan de Reus

ACNS: American Clinical Neurophysiology Society

IFCN: International Federation of Clinical Neurophysiology

WU-NEAT: Washington University – Neonatal EEG Analysis Toolbox

EDF: European Data Format

CSV: Comma Separated Value

PCA: Post Conceptional Age

PNA: Post Natal Age

GA: Gestational Age

Index

List of Figures

List of Tables

1 Presentation of the study

1.1 Objectives

The main goal of this work has been to compare the liquid gel electrodes currently used to perform amplitude integrated electroencephalography (aEEG), with a new electrode named aCUP-E (advanced cup electrode), specifically designed for aEEG recordings in the neonatal intensive care unit (NICU).

To achieve this main objective, it has been split into several sub-objectives.

(i) Define the importance of aEEG signal in the NICUs, highlighting the importance of a fast diagnosis, and identify the unmet needs regarding specific electrodes for aEEG.

(ii) Digitally create the aEEG signal, resembling the one seen on the monitor, from the raw electroencephalogram (EEG) data.

(iii) Determine the criteria to define optimal and non-optimal brain activity.

(iv) Determine the parameters to:
- Test if the electrodes of the two hemispheres capture similar signals when optimally recording.
- Quantify the performance of each electrode type.

(v) Define a statistical analysis to assess the differences between electrode types.

(vi) Apply the signal processing techniques to the recordings from the subjects of the clinical investigation conducted at *Hospital Universitari Sant Joan de Reus* (HUSJR).

1.2 Structure of the project

Below, the structure of the work is detailed, which has allowed us to achieve the objectives presented in the previous section.

In **2. Introduction** a presentation of the basic and essential concepts related to the project is made, together with its similarities and differences with other existing methods and its technical aspects. It will help to define some notions that will be used along the work, providing the necessary knowledge to delve into the topic.

In **3. Methods and Materials** the context in which the work was developed is presented. The new aCUP-E electrodes as well as the clinical research plan are detailed. The signal processing to convert the raw EEG into aEEG is also included in this section, together with the chosen parameters to characterize the data and the selected statistical analysis for each case.

Next, in section **4. Results and discussion**, the outcome of the analysis together with its interpretation is reported. The results compare either the signal acquisition of different hemispheres (within the same patient) or, between the different subjects of the clinical trial.

At **5. Conclusion,** where an overall assessment of the work is done, commenting on the general view of the analyses, and on additional work that could be done in the field.

Finally, in **Annex**, an extension of the results presented during the work can be seen. Mainly it refers to results from all the patients, since not all of them can be presented within the results and discussion section for the sake of clarity.

2 Introduction

Context - Why is it important to improve the techniques to monitor the brain activity of neonates?

In Neonatal Intensive Care Units (NICUs) neurological emergencies are a concern, both for clinicians and parents, at a level in which newborn neurocritical care requires dedicated expertise. Neurological pathologies account for 20% of current admissions to NICUs [1].

In the last years, neonatal monitoring has developed more precise and ergonomic tools to record functional parameters such as electrocardiogram (ECG), heart rate, blood pressure, oxygen saturation, and so on. This, along with other advances in the medical field, has led to an increase in the survival rate of newborns and preterm infants. However, not much has been done to improve the evaluation of brain function. So, despite the upgrades in other monitoring techniques, the neurodevelopmental problems that this population faces still remain [2].

As a result of the aforementioned, both neonatologists and clinical neurophysiologists agree that there is a need to improve the current techniques used to record brain activity [3]. Investing in these technologies is important because accurate and reliable monitoring of brain function can guide clinical decision-making, optimize treatment, and improve the overall care of critically ill neonates [4]. Early intervention can prevent or minimize neurological damage, decrease the likelihood of long-term developmental delays, and enhance outcomes. However, the acquisition must be accurate to allow the neonatologists to take appropriate decisions based on the data. In this sense, a misinterpretation due to interferences or disturbances (artifacts) in the recorded signal can have fatal consequences.

Current advances in brain monitoring are not suitable for newborns. Progress in electroencephalography acquisition has settled video-electroencephalography (vEEG) as a *gold standard* to continuously record and analyse brain activity from the cerebral cortex in real time. However, in NICUs, this method is not optimal due to the complex setting up and the long-lasting recordings with extended results, which require a 24h availability of neurophysiologists with special expertise in neonatal EEG [5]. Thus, EEG is more suitable for intermittent use, with recordings lasting from 20 minutes to several hours.

On the other hand, advances in medical imaging techniques provide a detailed anatomical evaluation of neonates' brain function and abnormalities. In spite of the fact that neuroimaging techniques are not continuous, it may help clinicians detecting injuries [3]. But, some of these techniques are time consuming and are susceptible to the movements of the neonates which makes them less suitable for infants.

Consequently, the scenario is settled for a new continuous monitoring technique to appear. In this context is where amplitude-integrated EEG (aEEG) arose. It is a technique that is nowadays used in NICUs around the world, and it is thought to be a more convenient method for continuous brain activity monitoring in neonates. Its main advantages rely on the fact that few electrodes are used, allowing cranial access to the nurses (fontanelles) and a quick assembly. However, it still has not been completely deployed into the clinics as a *gold standard* because there is a controversy between clinical practitioners about its interpretation [5] as well as some limitations to overcome, which will be discussed in this work.

2.1 Anatomy and physiology of the brain

The human brain is a subject of great fascination, as it holds immense interest due to its vast complexity and its questioned evolutionary significance. It is a complex organ that manages almost every body function, such as cognition, memory, emotion, or respiration.

The inside of the brain is characterized by regions of grey and white matter. These terms were given to different structures because of their appearance, which is strictly related to their composition. White matter refers to areas of the Central Nervous System (CNS) mainly made of myelinated axons, which provide a whitish colour due to the high lipid content of the myelin. On the other hand, grey matter contains neuronal cell bodies, glial cells, and non-myelinated axons. So, grey matter's role is to process and interpret the information, while white matter transmits that information to other sections of the nervous system [6].

Myelination is the process in which nerve cell axons are surrounded with myelin, that speeds up the conduction of the electrical impulses in the nervous system. Once the signal gets to the end of the neuron (axons), they communicate with each other thanks to synapses. These junctions can be either electrical or chemical. In the latter, there is a molecular machinery (neurotransmitters) that links the pre and the postsynaptic neurons [7]. The postsynaptic potential must exceed a threshold to trigger a response. One single transmission from the presynaptic neuron is too small to trigger the postsynaptic potential. Therefore, a nerve cell gets inputs from thousands of them, which can cause the activation of the impulse.

The electrical nature of the brain can be recorded due to the characteristics of the postsynaptic potentials, which are subject to a temporal and spatial summation of the inputs. Consequently, the produced signal is of longer duration and higher amplitude, which allows recording from distance. Due to this limitation with the separation between the electrical source and the recording electrode, current non-invasive brain monitoring techniques record the postsynaptic potentials of the cerebral cortex, which is the outer grey matter that covers the surface of the two cerebral hemispheres.

2.1.1 Neurodevelopment

At birth, the brain is not fully mature. The key period of brain development encompasses the last trimester of gestation and the early postnatal life. Within this time, both the cerebral cortex and the myelin sheath (oligodendrocytes) undergo different changes, giving the fundamental anatomical organization of the brain, and promoting the emergence of cognitive function. However, it is also at this time when the cortex is more vulnerable to perturbations, which can lead to cognitive deficits and adverse neurodevelopment [8].

White matter injury, usually due to inefficient myelination, has been considered the main pathology associated with preterm infants. So, myelination stands out for being a marker of maturation. This evidence was already mentioned by *Brody et al.* in (1987) [9], considering the state of myelin as a powerful tool to evaluate the maturation of the central nervous system (CNS) in autopsied infants. Nowadays, to assess it in vivo, magnetic resonance is the used modality to gain insight into the anatomical structure and growth of the brain [10]. Figure 1 shows the development at different gestation weeks.

Even though Magnetic Resonance Imaging (MRI) is a good technique to obtain anatomical information and map variations in tissue composition (myelin, iron, macromolecular content…) in early brain development [11] it is not optimal for neonates. Taking advantage of the electrical behavior of the brain, together with the proliferation of the cerebral cortex during neurodevelopment, electroencephalography techniques have been used to evaluate the brain activity and assess maturation.

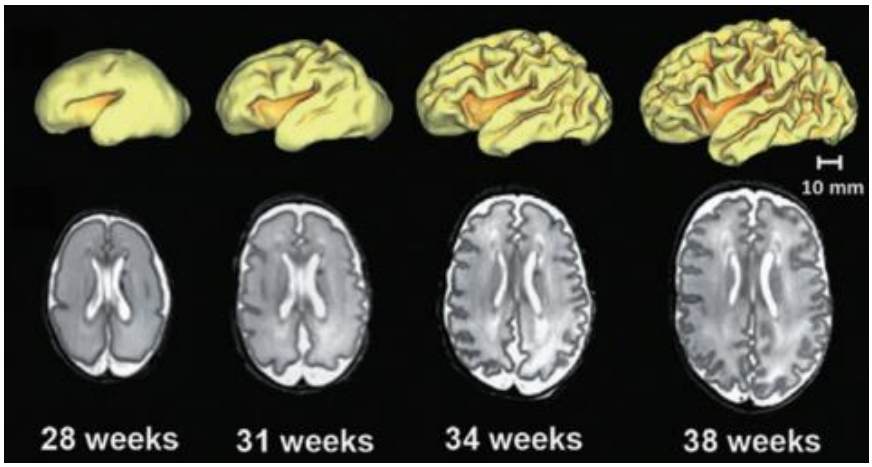

Figure 1: Growth and development of the preterm human brain. White matter as well as cerebral cortex maturation is seen. (Top) 3D reconstruction, (Bottom) MRI. [12].

The background pattern is the electrical activity observed in the brain when the subject is not engaged in any specific task. In newborns, this is the common case, and it is usually less organized due to the immature state of the nervous system. These activities allow seeing maturation patterns as well as underlying functional issues. Indeed, there is evidence of its potential and capabilities for prognosis when assessing the background activity in neonates [13].

With aEEG, this background activity can be visually evaluated in form of graphic patterns. These should be symmetrical in both hemispheres for neurologically healthy neonates due to the simultaneous maturation of the different neuronal populations of the brain [14]. The most common non-pathological pattern is the sleep-wake cycle, which presents a fusiform waveform. The narrower regions mean wakefulness or REM sleep, while the wider bands represent no REM sleep (or quiet sleep) (Figure 2). The proportion of time in each state depends on the maturation condition of the brain.

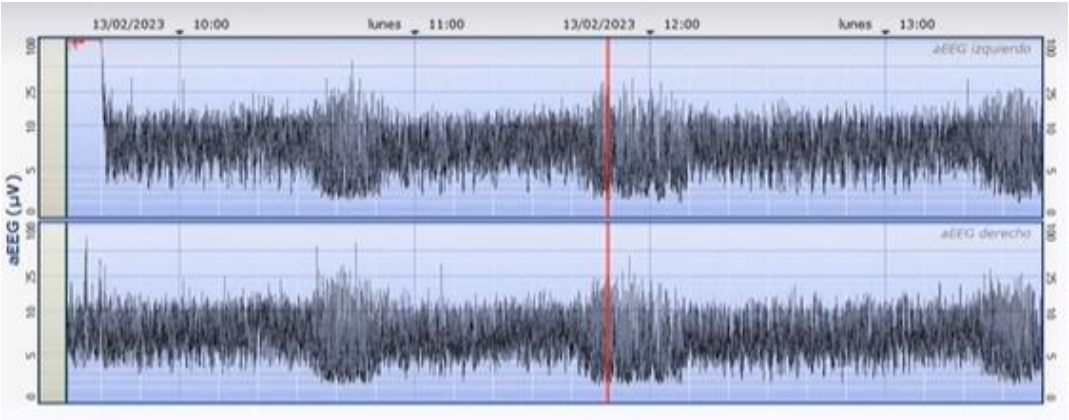

Figure 2: Sleep-wake cycle of a neonate (preterm, case 4). Wide band periods correspond to no REM sleep, while narrow periods correspond to REM sleep or wakefulness.

2.2 International 10-20 system

In order to properly evaluate the electrical activity of the cerebral cortex, the electrode positioning is an essential factor for both, clinical and research applications.

The 10-20 system is the method that has been internationally recognized by the American Clinical Neurophysiology Society (ACNS) and the International Federation of Clinical Neurophysiology (IFCN) as the standard for electrode placement. It was developed in 1958,

and the aim was to find a reproducible method to accurately place 21 electrodes on the corresponding underlying brain region [15].

The name of this system refers to the distance between neighbouring electrodes, being 10% or 20% of the measurements taken from the anatomical landmarks of the skull. The electrode position names are defined as letters, identifying the underlying brain region, and numbers, identifying the side (Table 1) [16].

Table 1: 10-20 International System nomenclature

	Nomenclature	Meaning
Lobe	Fp	Pre-frontal/frontopolar
	F	Frontal
	C	Central
	T	Temporal
	P	Parietal
	O	Occipital
Numbers	Even	Right hemisphere
	Odd	Left hemisphere
	Z (zero)	Midline

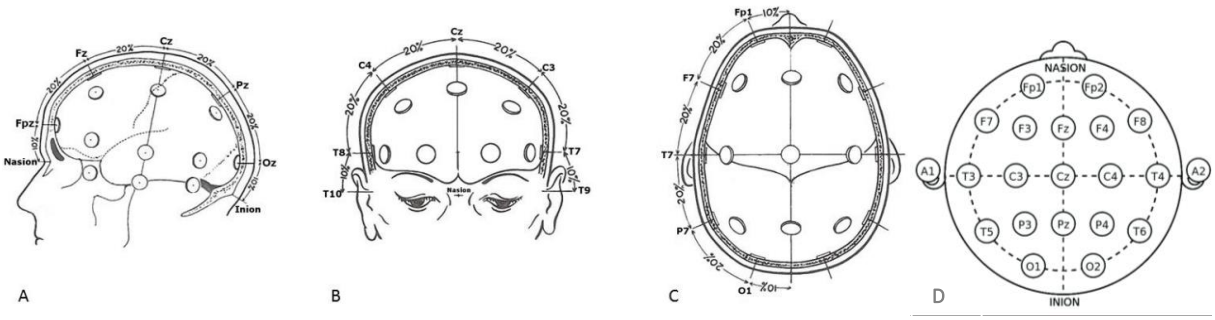

Figure 3: 10-20 International System. (A) Sagital Plane, (B) Coronal Plane, (C), Transverse Plane, (D) Electrode Position Scheme [16].

This system works with percentages or proportions (Figure 3), not with defined lengths. Therefore, it can adapt to different shapes and sizes. However, a defect of this method would be that a personalized calculation of the electrode positions must be performed for each patient due to the anatomical differences of the skull. Consequently, there has been a research line focused on trying to simplify this task.

The most common alternative to use the 10-20 system are electro-caps for multichannel EEG. These are elastic helmets with built-in electrodes. The elastic behaviour of the fabric theoretically allows the proportions of the 10-20 system to be respected and adapt to the cranial morphology of each individual. However, there are some techniques in which this solution is not suitable, due to the type of electrodes (e.g. needle electrodes), the

reduced number of electrodes required, the duration of the recording or the cranial size of the patient (e.g. neonates). In these cases, the nurses with experience still use the metric tape and calculations to mark the electrode positions, following a tedious and complex procedure to locate some specific positions from the 10-20 system.

Dr. Vicenç Pascual, Clinical Neurophysiologist at the Hospital *Universitari Sant Joan de Reus* realized that there was an unmet need related to the procedure of electrode marking system. Together with Dr. Albert Fabregat, from the Department of Mechanical Engineering of the *Universitat Rovira i Virgili*, created EPlacement, a device that guides the user through the steps to place the electrodes and simplifies the process. It measures the distance between skull landmarks with touch sensors and illuminates the points where electrodes have to be placed.

Despite that the 10-20 system is still the most used to provide guidance in electrode placing, advances in engineering have allowed EEG hardware to record a much higher number of channels simultaneously. Now, 10/10 and 10/5 systems are also used, which use the same skull landmarks but change the traditional proportions to fit more electrodes [15].

2.2.1 Adaptation to neonates

Neonates are fragile and there are more practical and technical limitations than in adults when placing electrodes on the scalp.

Newborns' skull is not completely formed, and it has soft membranous gaps between the cranial bones (fontanelles). This structure allows the deformation of the cranium during birth and a faster brain growth. Moreover, they are of great clinical significance because their size, shape, closure times, etc. can be strictly related to some pathologies. Thus, clinicians must be able to perform a thorough physical examination and get a detailed history [17]. For this reason, NICU health personnel must have access to the neonate's head while brain activity is being monitored, as there are various pathologies that can bulge the fontanelles. In addition, quality access to the epicranial veins is also required in NICUs, especially for preterm infants which physiologic and health status is compromised.

For these reasons, it seems obvious that the tendencies seen in adults are inappropriate for neonates. Smaller electrodes are needed, which do not damage the neonate fragile skin, and which allow for long-term recordings once precisely placed. A reduced number of electrodes with a more accurate positioning is required, rather than more electrodes to monitor. There is a need to adapt the 10-20 system to newborns, using fewer channels to monitor brain activity. Figure 4 shows the limitations of electrode positioning on the neonate's skull.

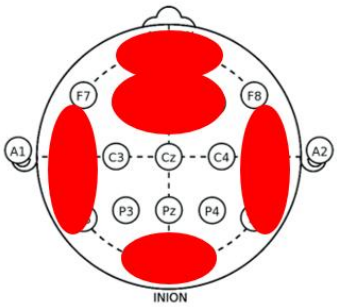

Figure 4: Limitations of the 10-20 International System when positioning electrodes on the neonate's scalp. It is necessary to avoid the anterior and posterior regions where the fontanelles are located; and avoid the temporal regions where the major temporalis muscles are located, which, when activated during suction movements, cause myoelectric artefact.

2.3 Amplitude-Integrated electroencephalography (aEEG)

2.3.1 Basis

Amplitude integrated electroencephalography (aEEG) is a method to monitor brain activity in neonates. The signal is derived from an EEG montage in which fewer electrodes are used. The number of channels is reduced and depends on the case of study as well as on the monitor. Some of them use a single-channel biparietal recording (as originally described) or more usually, two channels with two pairs of symmetric electrodes (P3-P4, C3-C4). The raw signal goes through a processing (detailed in 2.3.4 Signal Processing) which results in a compressed representation of the EEG (aEEG) [18].

The resulting trace is time-compressed (6 cm/h)[1] and represented on a semilogarithmic scale (linear 0 - 10 mV, logarithmic 10 - 100 mV). The signal's amplitude defines two bands that reflect variations of the EEG amplitude. One band is called the lower margin and corresponds to the low-voltage activity. The other, called the upper margin, is related to the high-voltage activity.

This evolution of the margins is what will be used to identify pathological patterns. The semilogarithmic scale allows enhancing changes in low voltages, without giving much importance to high-amplitude changes. Additionally, the time-compression provides an overview of the long-term trends of the cerebral activity.

This technique uses fewer electrodes than the conventional ones (EEG), so it has less sensitivity. One of the ways to overcome these limitations is what current monitors do, displaying and storing the EEG signal. This allows clinicians to clarify their doubts and facilitates the artefact recognition. Moreover, in recent equipment, the electrodes' impedance is also continuously recorded and can be displayed by switching the EEG signal with easy touchscreen commands.

What has just been stated above, can be seen in Figure 5. The aEEG (top) represents more than four hours of recording, while the raw EEG (bottom) corresponds to thirty-four seconds. The lower and upper margins can be seen above, as well as the effect that the high and low EEG amplitude have on the trace.

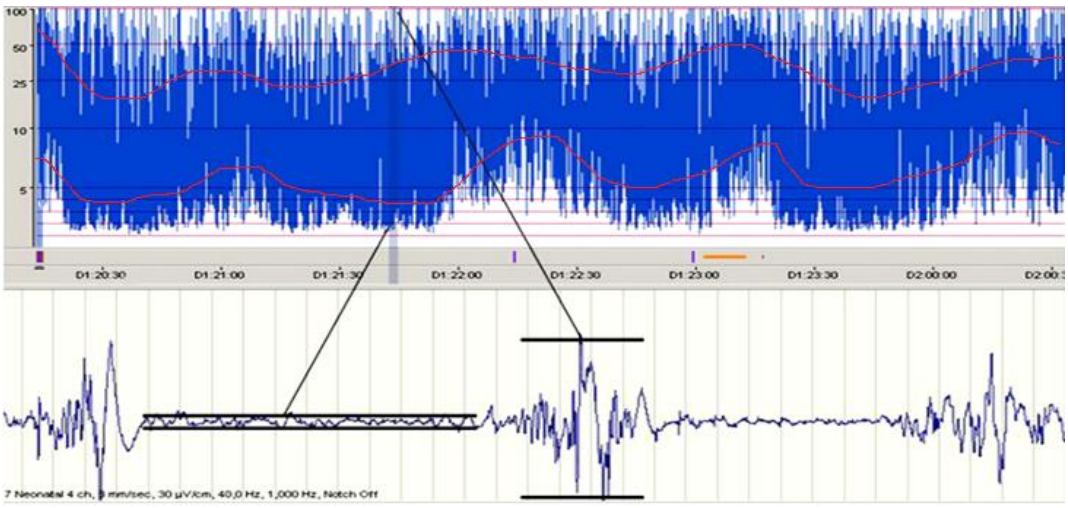

Figure 5: >4 hours aEEG channel (above) with the corresponding 34s of raw EEG of the selected region of interest (below). Upper on lower margins have been manually added on the original image. [18]

[1] In this work, the x-*axis* ratio is not conserved, since the images size are limited to the width of the paper sheet.

2.3.2 State of the art

The monitoring of neonate's brain activity is a clinical tool that has been used in NICUs for several decades, without any consensus protocol. However, recent advances in medicine and engineering have underlined its importance and increased the interest over the world. In this section, how aEEG was introduced into the clinics and its current challenges will be presented, together with the barriers that other techniques present.

The first device for amplitude-integrated electroencephalography, previously called Cerebral Function Monitor[2] (CFM), was originally developed in 1969 by *D. Maynard* and *P.F. Prior* [19]. The aim was to use it in patients who had resuscitated from a cardiorespiratory arrest to accurately diagnose possible brain damage, together with conventional EEG to assess the probability of survival.

The authors detailed the general principles of cerebral function monitoring, which have evolved slightly up to now. CFM was described as "a system in which the EEG signal from a single pair of electrodes is amplified and passed through a special wide-band filter" [19]. Furthermore, emphasis on the importance of good adherence for extended recordings was already placed by the authors at that time. For this reason, an electrode impedance monitor was added in parallel to the CFM system (Figure 6). About the brain monitoring path, the radio frequency trap was used to eliminate the static electricity interference. Then, the signal was passed through a special EEG filter whose aim was to flatten the spectrum because not all frequencies are equally attenuated through the scalp. Finally, the signal was compressed and displayed in a logarithmic scale.

CFM was designed as an analogical equipment, but modern methods are digital. The original concepts and advantages have been kept as well as the CFM-like signal (currently called aEEG), which now is digitally built from the EEG trace [20].

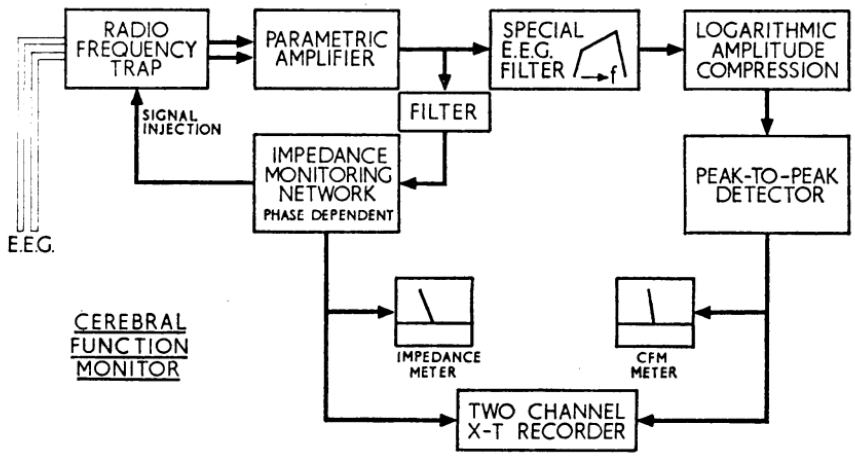

Figure 6: Block diagram of cerebral function monitor (right branch) with impedance monitor (left branch). 1969 [19]

Two years later, in 1971, *D. Maynard* and *P.F. Prior* [21] performed a clinical experience recording the electrical activity of the brain, providing information about the state of cerebral activity for long periods. The aim was to assess the cerebral function monitor device over conventional EEG, which had some limitations because it was costly in terms of apparatus and the results were too long, which required the continuous operation of

[2] This technology was originally known as Cerebral Function Monitor (CFM), but the later digital versions are commonly called aEEG [20]. In this section, both words are used interchangeably, but the chronological order of appearance in the literature is conserved.

specialized personnel. These obstacles remain nowadays, but when this research was done, they were still working with paper rolls, which made the task of review and diagnosis even more difficult. In Table 2, a comparison between conventional EEG and CFM technologies in the year 1971 is displayed.

Table 2. Comparison of CFM (aEEG) and conventional EEG Apparatus (1971). [21]

	EEG	CFM (aEEG)
Apparatus	- Costly - Bulky but transportable - Lengthy: 180 cm/hour Recording during cardiac operation about 300-600 meters long - Requires expert eye for interpretation	- Relatively cheap - Small and portable - Compressed brief record: 2.5-36 cm/hour. Recording during cardiac operation about 1-2 meters long - Easy to detect sudden or gradual trends to increase or decrease of activity or stable record
Recording techniques	Interference a problem	Interference automatically excluded
Use		
Patients with generalized disturbances of cerebral function	Suitable	Adequate
For determining absence of cerebral activity	Satisfactory	Should be used in conjunction with intermittent EEG
Patients with localized cerebral abnormality	Useful for detecting focal disturbances	Not designed to detect focal disturbances

Within these clinical trials [21], the CFM device showed to be of value in three circumstances:

- During open heart surgery, when cerebral circulation is likely to be vulnerable.
- As a measure to follow the evolution of brain damage (e.g. after cardiorespiratory resuscitation).
- In cases in which information about more physiological changes in cerebral function is required (e.g. know the depth of anesthesia for a test or in a surgery).

However, all these applications are focused on post-anoxic or post-traumatic coma in adults. In 1983 *I. Bjerre*, together with *L. Hellström-Westas* (one of the top authors on newborn aEEG) were the first to adapt this technique for neonatal use [22]. The aim of this clinical research was to estimate the value of CFM in preterm and term infants who have had episodes of hypoxia. Its diagnostic and prognostic capabilities in NICUs were shown, having the potentiality to reduce the number of intermittent EEG recordings, but they were still necessary.

At that point, the research focused on trying to compare aEEG with conventional EEG and find evidence regarding its contribution to neonatal neurological disorders. The aim was to define normal and abnormal patterns for the diagnostic and prognostic accuracy of aEEG.

To do so, some of the few studies relied on subjective visual recognition of patterns, but *Al Naqeeb et al. (1999)* [23] focused on defining the normal values and test the interobserver variability, for which no data was found at that moment. The results showed that the doctors had no problem in assigning scans to different categories (interobserver

reliability) and defined a simple scale based on the amplitude margins to evaluate the severity of the encephalopathy of term infants.

In 2006, *Hellström-Westas et al.* [18] suggested a new classification on aEEG tracings in order to have a unifying nomenclature that englobes term and preterm infants. The classification was based on both, amplitude margins and pattern recognition, and it is still used nowadays (Figure 7).

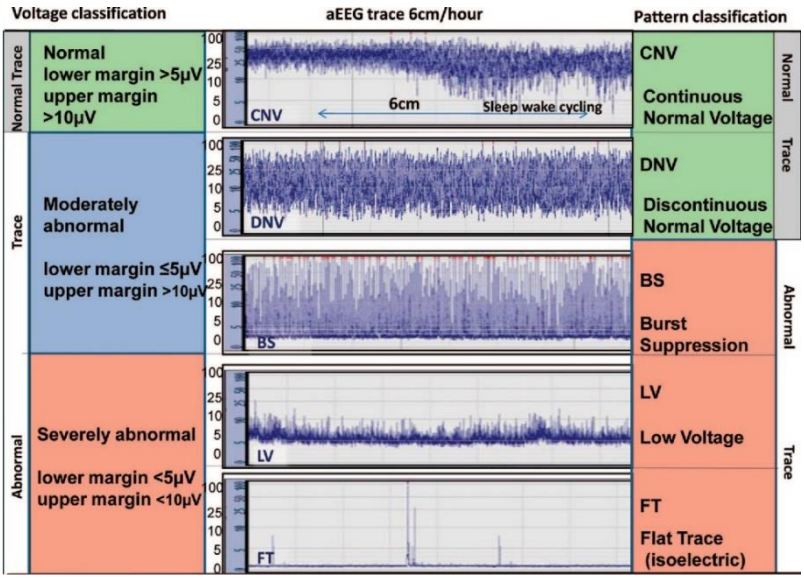

Figure 7: Hellstrom-Westas Scale. On the left, the classification by amplitude (voltage) margins, on the right, the classification by pattern recognition. Both are complementary and help on clinical decisions.

The current research has not changed much. In recent years, the focus has been set to compare the use of EEG/aEEG in Hypoxic-ischemic Encephalopathies (HIE), neonatal seizures, and preterm outcome prediction (prognosis) [20]. The aim is the early detection of any brain disfunction in order to be able to effectively apply the corresponding treatment, which will end up in an improvement of the neonate's neurodevelopment.

For neonates with HIE, candidates for therapeutic hypothermia (TH), time factor is decisive since it is considered effective when applied in the first 6 hours of life. This recent treatment (early 2010s in Spain) consists of moderately lowering the patient's body temperature and is crucial to reduce/delay the possible neurological hindrances as well as to improve the prognosis. Hypothermia treatment is based on putting neurons in a state of minimal metabolic consumption to minimize neuronal death in neural tissue subjected to ischemic and/or hypoxic restriction. So, in this field, the main power of aEEG relies on helping to take rapid decisions in the first hours of life, what would be beneficial for the infant [20]

L. Hellström-Westas et al. already published research about this in 1995 and concluded that the early use of aEEG monitoring after birth asphyxia (case of HIE) seemed to be suitable for the identification of the brain damage risk. Their findings indicated that monitoring during the first 6 postnatal hours has enough good predictive capability to enable physicians to make invasive decisions (TH still not used).

Nevertheless, more recent studies in HIE are focused on gaining insight into therapeutic hypothermia: the evolution of the background activity for prognosis as well as the optimal temporal window of the treatment.

Del Río et al. [24] performed a study comparing different aEEG recording epochs and concluded that monitoring during the first 72 hours of life of infants with HIE treated or not with hypothermia has a strong predictive value, and that a longer lasting recording won't significantly improve the prognosis. Also, this study demonstrated that applying TH slowed down the evolution of brain damage. A more recent review (2020) conducted by *Ouwehand et al.* [25] comparing the most currently used neurophysiologic and neuroimaging techniques for the prediction of neurodevelopmental outcomes following TH on HIE infants, states that among all methods, aEEG at 36 h has the highest Diagnostics Odds Ratio (DOR, equation (1)).

$$\mathrm{DOR} = \frac{TruePositives * TrueNegatives}{FalsePositives * FalseNegatives} \quad (1)$$

Emphasis has also been placed on Neonatal Seizures (NS), particularly in critically ill neonates because it has poor clinical or motor manifestations and needs a prompt treatment. Usually, NS are caused or related to other severe conditions such as hypoxia-ischemia, cerebral hemorrhage, metabolic disturbance, and infection. Therefore, continuous monitoring of brain activity is necessary to be able to detect them.

In 2009 it was estimated that only half of the clinical seizures were correctly classified and that NS diagnosis methods vary among centers [20]. So, it seems that there is an urgent need to reach a consensus to guide seizure detection in newborn infants.

A systematic review of the previous literature conducted by *Rakshasbhuvankar et al.* [26] concluded that the aEEG specificity (true negatives ratio) and the sensitivity (true positives ratio) from the selected seizure studies were relatively low and variable. This is due to the reduced number of electrodes that facilitate the handling of ill neonates. This aEEG advantage is also what can cause focal seizures to go unnoticed, because fewer channels means that the brain activity can not be precisely located [27]. This may be one of the main reasons why conventional EEG is still the *gold standard* for seizure detection. However, two channel cerebral function monitoring with a simultaneous display of the raw EEG can be used as a screening tool, using multichannel EEG to clarify any doubts [20], [27].

To solve the problem of seizures going unnoticed, automated seizure detection algorithms (SDAs) for neonates have been developed during the last years. These methods aim to reduce the amount of necessary EEG electrodes and recording time. First generation methods, already in 1992, were developed as an adaptation of adult's SDAs. The second generation (1998 to 2012) involved more advanced methods to extract features from the EEG. Finally, the third generation used modern techniques such as wavelet analysis or machine learning algorithms, trained using large databases [27].

However, the implementation of SDAs into the clinic is slow because of the uncertainty regarding the collected information and the overall assessment of SDAs on common data [27]. To develop these techniques, it is necessary to identify on the data what constitutes a seizure and what does not, using the neurologist's or clinical neurophysiologist's visual interpretation of the EEG. Even so, to overcome the limitations that aEEG has in seizure detection some modern monitors incorporate SDAs to assist in seizure detection, yet supervision by clinicians is always needed [20].

Another topic that is causing concern in neonates' brain monitoring is the electrodes. A proper electrode could help improve the acquired signal, reduce noise, and help both EEG and aEEG to overcome some of its limitations. Moreover, neonates are fragile, and they will be subjected to long-lasting recordings. Therefore, the electrodes should adapt to these particularities of the test. To do so, parameters such as skin preparation, risk of skin damage, speed of placement, electrode replacement, longevity of the electrode, etc. should be evaluated [28]. Nowadays, the most suitable ones are self-adhesive electrodes with

liquid gel because of their quick placement and non-invasiveness. Nevertheless, there are still several challenges to overcome, which are of interest for this study.

2.3.3 Research trends

To analyse the different trends of amplitude integrated EEG research, *The Lens – Free & Open Patent and Scholarly Search* (*lens.org*) has been used as a scholarly and patent discovery tool. It is a recent service owned by non-profit Cambia, that goes beyond other citation tools by allowing us to perform a deep analysis with user-friendly visualizations. It has a large database of scholarly records from other sources such as *Pubmed* or *Microsoft Academic* together with patent records.

These characteristics, make this tool suitable for the purpose of this research: study the trends related to aEEG.

With the query: *(aEEG) OR (amplitude integrated EEG) OR (cerebral function monitoring)* on the fields *Title, abstract, Keyword and Field of study* a wide search is done, in which 5766 scholarly works are obtained. The evolution (Figure 8) corresponds to what has been seen in the state of the art. In 1969, the CFM device is published. Since then, the tendency has grown exponentially, having the turning point between the years 2000 and 2010, when therapeutic hypothermia first began to be used in clinics.

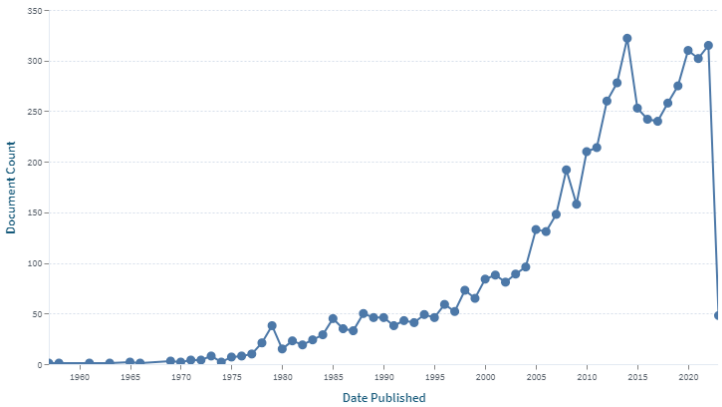

Figure 8: Number of scholarly works over time (*lens.org*)

To perform further analysis, only the ones published after 2010 will be selected. This date is not arbitrary since it is when therapeutic hypothermia was introduced (in Spain) and changed the aEEG paradigm. With this filter, 3257 articles are obtained.

The top institutions by Document count since 2010 are the ones detailed in Figure 9. The Boston Children's Hospital is the institution that is investing in further research on this field, doubling the number of works published by the following organization (Harvard University).

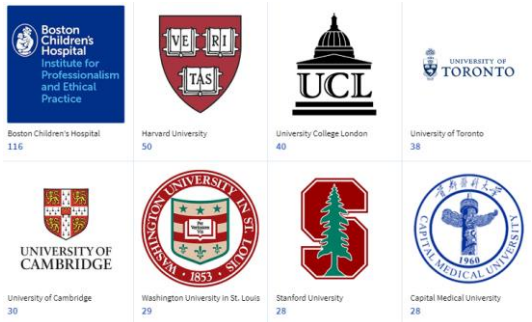

Figure 9: Top institutions by document count (*lens.org*)

It should be noted that this search is very broad. If we reduce only to neonates: (*(aEEG) OR (amplitude integrated EEG) OR (cerebral function monitoring)) AND (newborns OR neonates)* we get 683 scholarly works after 2010.

Lena-Hellstron Westas is the top author for neonatal aEEG. She was one of the first scientists to bring this technology to neonates already in 1983. She has dedicated his life to understanding and improving the limitations that it has in the clinics. To do so, she has published more than 45 articles, which have a significant number of citations. Also, G.B Boylan, M.C Toet, F. Gronendaal, are other authors that have done research regarding aEEG in specific applications. Its contribution to the field is also notorious.

2.3.4 Signal Processing

The aEEG signal processing has not changed much from what D. Maynard and P.F. Prior defined in 1969 [19]. Even so, the digitalization process affected the amplitude integrated EEG instrument in such a way that the aEEG signal is nowadays digitally derived from the raw EEG. However, this transformation has only been well described in pure analog prototypes and information about the digital models has not been disclosed. Yet, the principles must be the same ones [29].

The human brain activity is composed of waves that attenuate at a different rate while being transferred through the skull and scalp. This loss of signal depends on the frequency of oscillation and is due to the capacitive behavior of the biological structures between the electrode and the brain. To give an equal weight to all frequency components the aEEG signal processing uses an asymmetrical filter with a slope of 12 dB per decade in the range of 2-15 Hz, which is the one of interest. A 60 dB/decade is used between 0-2 Hz and a -120 dB/decade is used to attenuate frequencies > 15 Hz (Figure 10) [30].

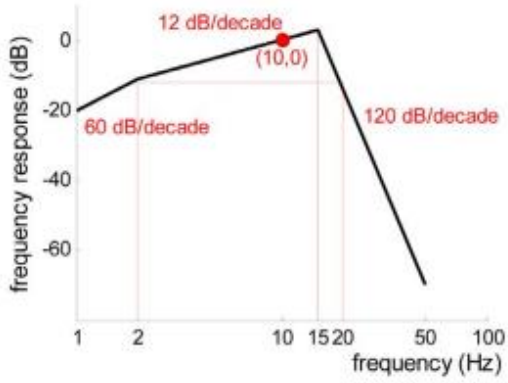

Figure 10: Frequency response of the analog filter [30]

To detect the amplitude trends of the brain activity, first the signal has to be rectified in order to detect the amplitude of the positive and negative peaks, since the EEG is a biphasic signal. In the analog mode, a full-wave rectifier is used, which is similar to the absolute value of the signal.

The las step is detecting the envelope. It is the one in which more discrepancy is found, because the definition of envelope is ambiguous and without exact mathematical description. The envelope is *'an estimation that follows closely sudden variations in amplitude and avoids ripples in more stable regions'* [29]. Different algorithms are proposed to smooth the amplitude of the rectified signal, such as low-pass filtering, moving average or the Hilbert transform (mathematical function to compute the analytical signal).

Figure 11 sums up the process to obtain the aEEG signal.

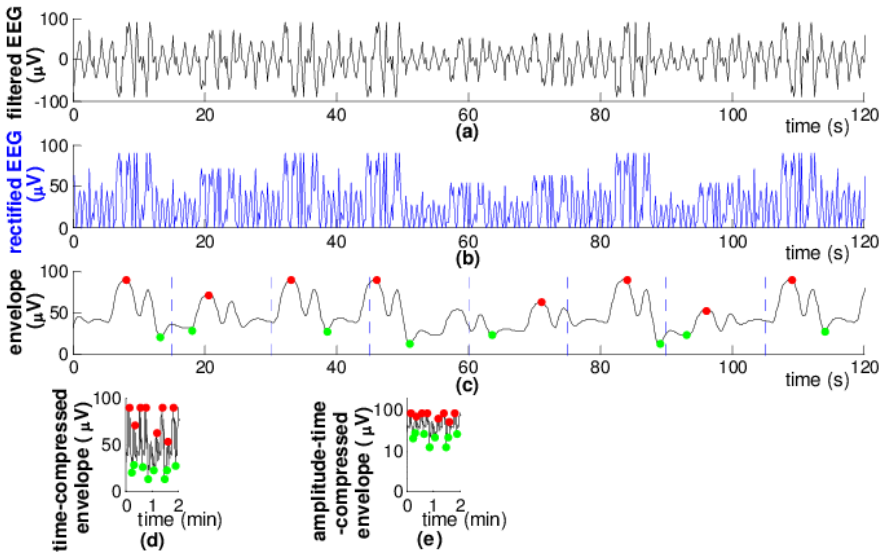

Figure 11: Workflow to obtain the aEEG signal. (a) Asymmetrical filtering, (b) Rectifying, (c) Envelope detection, (d) time-compression, (e) Semi-logarithmic scale [30].

To have a wider view of the brain activity, the obtained signal is now time-compressed (x-*axis*). The compression procedure of the time follows a reference scale of 6 cm/h. This strategy reduces the longitude of the recording to evaluate in comparison with the *gold standard*, in which the reference scale is between 15-30 mm/sec (5400 -10800 cm/h). At last, the signal is compressed in a semilogarithmic scale (y-*axis*), in which the voltage between 0-10 μV is linearly displayed and between 10-100 μV is logarithmically displayed. This procedure allows enhancing the changes in low-voltage activity and reduce the range of fluctuation of high amplitudes, allowing a better recognition of the variations of interest [29]. Figure 12 shows a fragment of an aEEG signal, in which this features can be seen.

Figure 12: aEEG signal of one hemisphere from the *CFM Olympic Brainz Monitor*. Semilogarithmic scale is observed, as well as time-compression. The distance between each white vertical line is 10 minutes.

2.3.5 Impedance concept

The concept of impedance is the opposition to alternating current presented by the combination of resistance, inductance, and capacitance. When translating it into clinical neurophysiology techniques, it is highly related to the skin-electrode contact. Scalp or skin impedance depends on different factors such as hydration, epidermis fat layer, amount of hair… In neonates, the impedance of the skin has been presumed to be lower due to a higher hydration of immature skin. However, skin preparation is still needed to obtain a good recording [4].

The characteristics of the surface electrodes for bipotential recordings has been already modelled by a non-linear RC circuit, whose components are frequency and current dependent [31]. Figure 13 shows the skin-electrode interface. To improve the impedance, we can only manipulate the outer layers, hence, cleaning of the epidermis to avoid sweat

and fat as well as a good contact between the electrode and the surface are sought when talking about skin preparation. Needle electrodes skip this scheme, going directly to deeper tissues and therefore having better impedance. On the other hand, they are invasive and not recommended in neonates.

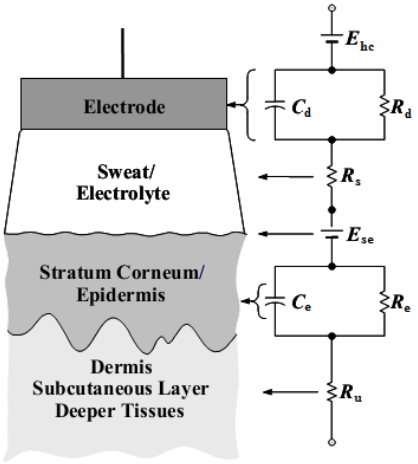

Figure 13: Generalized model of the electrode-skin interface. From R_S above is what is called electrode-skin contact.[31]

When analyzing the previous circuit (Figure 13), various layers are observed to hinder the flow of the electric current generated by the brain. From the bottom to the top, the dermis and deeper layers are first found, which in general are pure resistance (R_u), not changing with the frequency. The epidermis is frequency dependent. At higher frequencies, $1/(wC_e) \ll R_e$, there will be a short-circuit and the impedance will be almost neglected due to the low resistance that the capacitor-like behavior gives. However, at lower frequencies $1/(wC_e) \gg R_e$ (open circuit), where the impedance of this phase will be constant at R_e [31]. Frequencies between these two extremes will make this impedance to be frequency dependent (Figure 14).

The skin surface is considered a semipermeable membrane (such as the cellular membrane), in which a potential difference exists. In the previous image this is represented with E_{se}. The electrolyte also supposes a constant resistance R_S, while the electrode-electrolyte interface is frequency dependent. E_{hc} is the half-cell potential, which is a characteristic of the electrodes when subject to an electrochemical reaction (Redox).

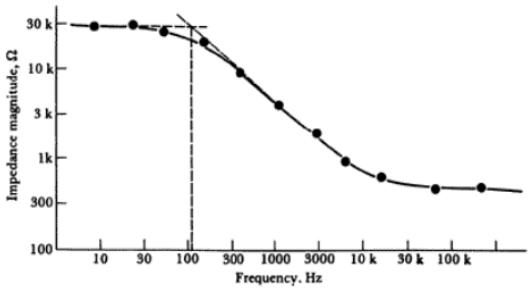

Figure 14: Variation of electrode impedance with frequencies [31].

Once the electrical scheme of the electrodes has been introduced, a closer examination can be conducted regarding the impact it has on aEEG. This technique is based on a bipolar montage where the difference between the signals captured by the electrodes in one hemisphere is amplified thanks to a differential amplifier (usually instrumentation amplifier) [32]. In Figure 15, the differential amplifier output is the difference between the signal

detected in A" minus the signal detected in B". In the extreme where just one electrode detaches (A), this point won't receive brain activity and the output of the differential amplifier will be -B" (neglecting noise capture). So, the resultant signal, which is the raw EEG, is more relevant as more similar are the impedances of both electrodes. This is because when they differ, the two captured magnitudes (A" & B") are not equally related (different attenuation) to the brain activity, and the difference may be influenced by impedance bias.

Moreover, high electrode impedances increase the susceptibility of the measurement system to capture noise typical from the clinical environment such as lighting, ventilation, computers… Ideally, electromagnetic interferences (EMIs) should not have any effect because of the nature of the instrumentation amplifier, that cancels out same input's voltages in both entries. This is known as *Common Mode Rejection Ratio* (CMRR) and depends on the quality of the amplifier (usually above 100 dB for EEG) [32]. Nevertheless, when the montage presents different impedances the amount of noise detected by each electrode won't be the same, hence the CMRR won't work efficiently, leaking some undesired artifacts in the bipolar raw EEG.

In Figure 15, the difference in potential between A or B and A" or B" is what must be reduced in order to achieve the two described requirements: lower and stable impedance in both electrodes of the hemisphere. To achieve it, skin preparation, electroconductive gel and electrode design are key factors.

Ideally, the impedances should be equal in all the electrodes in an aEEG montage to efficiently compare both hemispheres. However, since this is a difficult task, nowadays monitors continuously record the impedances so that clinicians can assess the differences between the signals taking this into account.

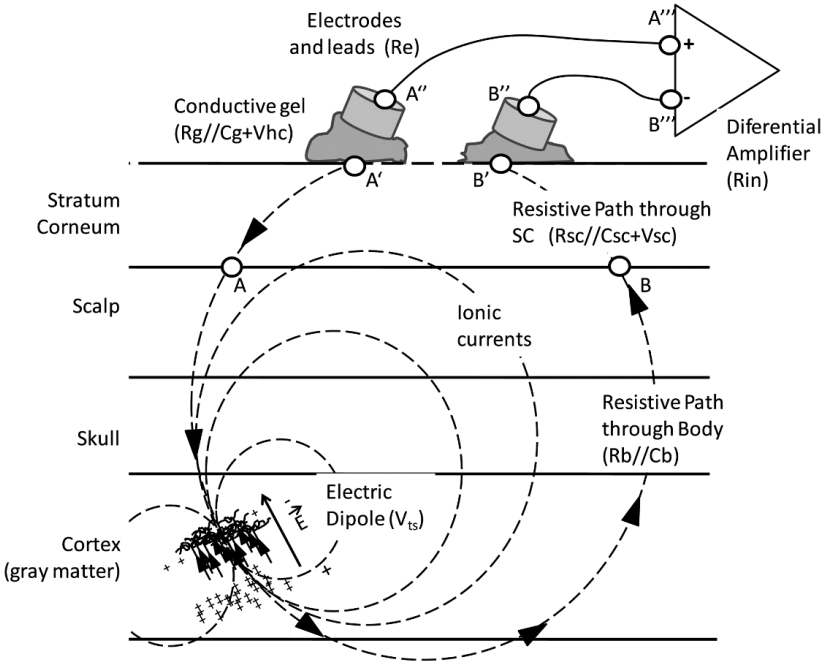

Figure 15: Scheme of electric dipole, ionic currents, and the measurement of the brain activity by the electrodes together with the differential amplifier [32].

2.3.5.1 Epilepsy simulation

Epilepsy simulation is one of the main clinical concerns when using aEEG in the NICUs. As stated above, this technique aims to quickly diagnose different encephalopathies in which time is a decisive factor. In this context, the methods should be precise enough to not lead to any false positive, where the treatments are applied to healthy subjects.

In neonates, doctors seek for seizure signs that may lead to the diagnosis of HIE or epilepsy. Figure 16 shows a real case of epilepsy, in which an increase on the voltage is seen in the aEEG, together with characteristic discharge pattern [2].

On the other hand, Figure 17 shows a simulated case of epilepsy on the left hemisphere (top row of aEEG and EEG). If clinicians only had the aEEG, they could easily be confused due to the increase of the voltage, which is similar to the one in the previous figure. However, when assessing the corresponding EEG no epilepsy patterns are found, being considered as artifact.

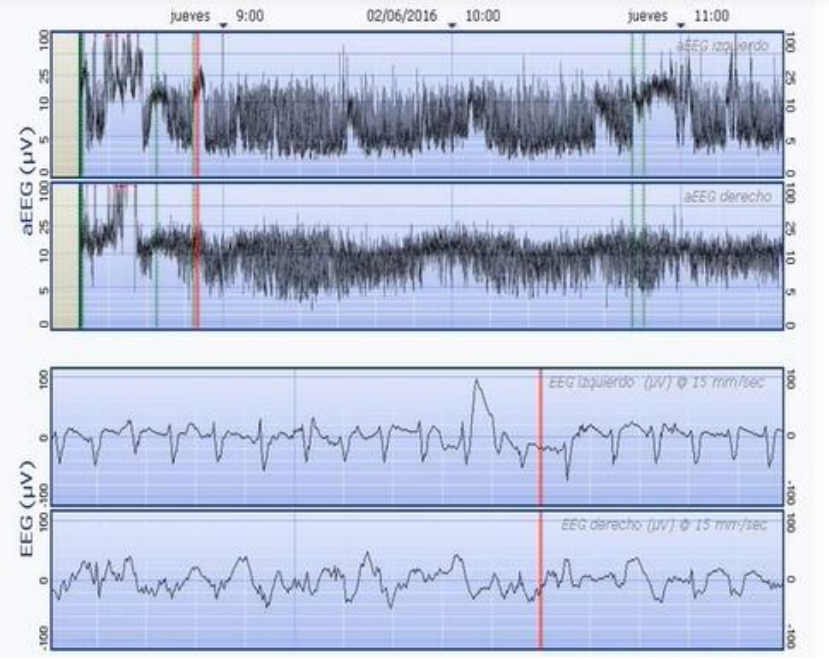

Figure 16: Shows a real case of epilepsy at the point where the cursor is placed on the left hemisphere aEEG. Top and bottom signals of both aEEG and EEG relate to the left hemisphere, while the bottom ones are the right hemisphere.

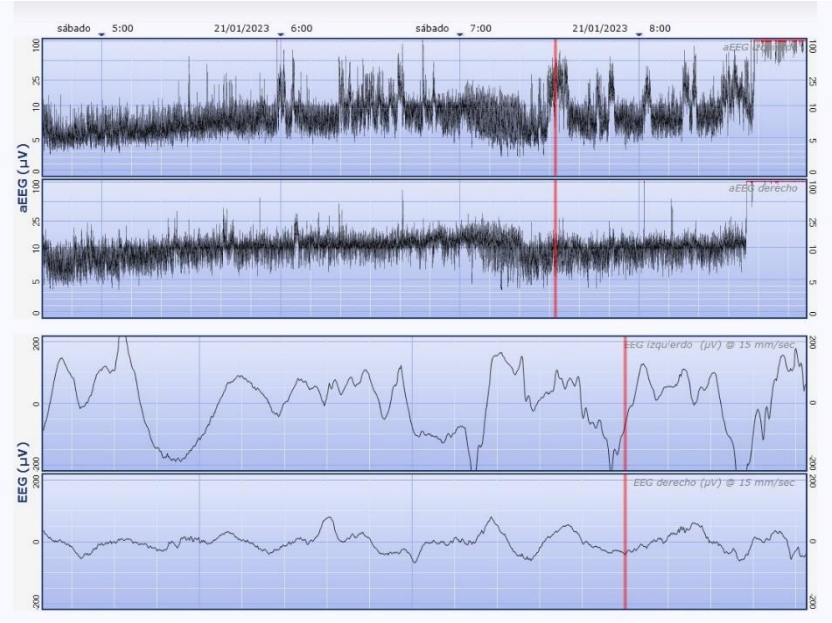

Figure 17: Simulation of an epilepsy at the point where the cursor is placed on the left hemisphere of the aEEG. Top signals of both aEEG (above) and EEG (below) relate to the left hemisphere, while the bottom ones are the right hemisphere.

This epilepsy simulation is strongly linked to impedance stability. As shown in 2.3.5 Impedance concept, when only one of the electrodes has a poor contact, the output of the differential amplifier will be larger, because the signal coming from both electrodes is not evenly related to the brain activity (more different). In the aEEG, this is translated into an increase of the voltage (lower and upper margin), which is not due to brain activity [32]. Therefore, it can simulate epilepsy even though the subject is in healthy conditions. Figure 18 illustrates the effect of impedance variability (electrode detachment, gel drying, wire movements …) in the aEEG. The impedance (bottom) graph is the maximum value between the two electrodes of the hemisphere; hence an increase may be related to just one bad skin-electrode contact.

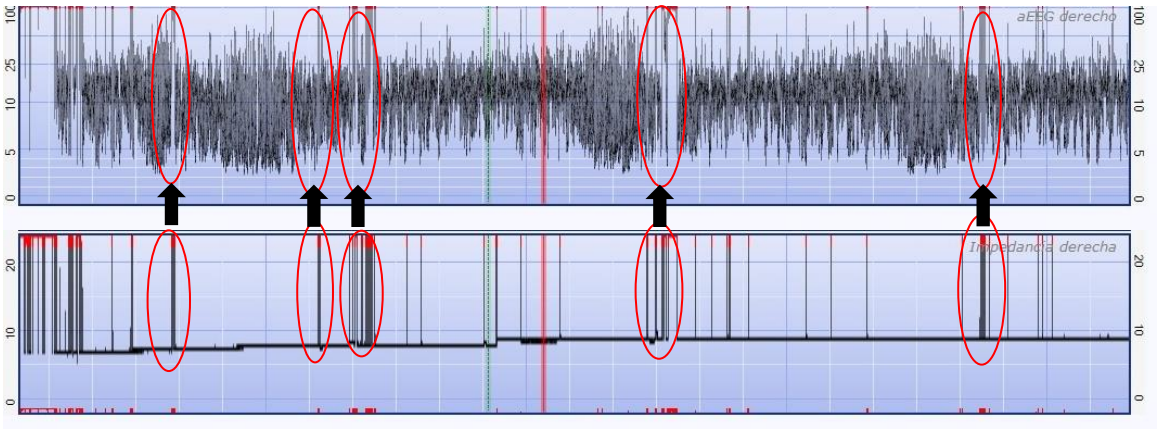

Figure 18: Red circles show the effect of an impedance spike, which leads to an increase of the aEEG voltage, which could simulate a seizure. (Top) aEEG, (Bottom) Impedance.

As demonstrated, these variabilities of the impedance between electrodes of the same hemisphere may cause voltage changes or a reduction of the sensitivity, which may lead clinicians to make an error with bad consequences for the healthy neonates (false positive). Consequently, electrodes are a key factor for this technique, and there are still some challenges to overcome, such as impedance stability [4].

3 Methods and Materials

3.1 Electrodes

3.1.1 aCUP-E

Dr. Vicenç Pascual, clinical neurophysiologist at the *Hospital Universitari Sant Joan de Reus* recognized the shortcomings and issues that adult electrodes present when applied to neonates: primarily big dimensions and poor adhesion. Moreover, none were found that fulfilled the desired requirements, such as adapting to the curvature of the head or having a good attachment. Hence, together with Dr. Albert Fabregat from the Department of Mechanical Engineering of the *Universitat Rovira i Virgili,* developed an electrode that met the needs and adapted to the specific situation of newbors.

Advanced Cup electrode (aCUP-E) is the new electrode designed specifically to fit the necessities of neonates long-lasting monitoring in the NICUs. It is flexible, with a firm adhesion and safe for the fragile skin of the neonatal scalp. Its use is indicated for cases in which long studies are required, as it shows good adhesion, easy replacement of the electroconductive gel, keeps a stable impedance, and allows a comfortable manipulation of the newborn by the healthcare personnel (Figure 19).

Specific details of aCUP-E electrode are not explained because of the intellectual protection, although they are not relevant for this study either. However, Figure 19 shows and scheme or the aCUP-E electrodes.

Figure 19: a-CUP electrode scheme. (1) Universal connector, able to connect to all EEG devices. (2) Coil of wire to facilitate movement without detachment. (3) Opening to introduce the gel, with its cover to avoid electroconductive gel spill. (4) Adhesive for delicate skins, long recordings, and good adherence.

3.1.2 Neuroline720

Neuroline720™ electrode from Ambu® have been used as the commercial type in this study. They are liquid gel electrodes, which are considered to be the best for neonatal monitoring [28], [33]. They are self-adhesive and have already embedded the electroconductive gel in a sponge. It has a size of 30x22 mm and the area of measurement is 95 mm^2. The electrode plate is covered with Ag/AgCl (Figure 20).

In the images as well as in the text, these electrodes will be referred to as commercials.

Figure 20: Neuroline720 electrode from Ambu®. [*Ambu® Neuroline™ 720*. *Ambu Forever Forward*. Available at: https://www.ambu.es/neurologia/electrodos-emg/producto/ambu-neuroline-720]

3.2 Clinical research plan

This work has been performed in the framework of a clinical investigation that was being conducted at *Hospital Universitari San Joan de Reus* by Dr. Vicenç Pascual Rubio. This work and the clinical trial developed simultaneously, which allowed a better understanding of the process and the data obtained. The protocol of the clinical investigation plan was already designed at the start of this project, but it is detailed in the following sections to better understand and contextualize this work.

3.2.1 Objective

Compare the new electrode, aCUP-E (advanced cup electrode), specifically designed to perform amplitude-integrated electroencephalography (aEEG) in the neonatal intensive care unit (NICU); with the liquid gel electrodes currently used in *Hospital Universitari Sant Joan de Reus* and recommended by the centres with more experience in aEEG. These commercial electrodes are Neuroline 720, from Ambu®.

3.2.2 Hypothesis

The new aCUP-E electrode has the same safety and quality of the bioelectric signal compared to liquid gel electrodes. It has the advantages of good adhesion, a stable impedance (reducing the number of artefacts), a more comfortable handling of the newborn by healthcare personnel, and the ability to replace the electroconductive gel, that allows long-lasting recordings without removing the electrode.

3.2.3 Description of the study

A clinical and diagnostic trial will be carried out on 20 newborns at the *Hospital Universitari Sant Joan de Reus*, classified into two groups: 10 term and 10 preterm.

An aEEG analysis during the time the neonates are in the NICU will be performed. The two different types of electrodes will simultaneously be used in the recording sessions. Thus, one hemisphere will be recorded with liquid gel electrodes and the other with the aCUP-E. Data on ease of placement, removal and convenience will be collected for each type of electrode; the comfort in handling the newborn by healthcare personnel; the number of relocations of the electrode during recording; the number of times electroconductive gel is applied to aCUP-E, the quality of the recording and the safety of the newborn's skin.

The recording will only be performed to those subjects that meet the inclusion criteria, in which no suggestive signs of neurological damage can be seen.

3.2.4 Electrode placement

Electrodes have been placed following a bipolar montage with 5 electrodes that considers the constraints of neonatal brain monitoring. The used positions, regarding the 10-20 system, are C4 and P4 (right hemisphere), C3 and P3 (left hemisphere) and Cz as the reference electrode.

A pair of each type of electrodes (aCUP-E and liquid gel) have been placed on each hemisphere. For the reference, an aCUP-E electrode has also been used. The latter does not record any activity and acts as a ground. This image has been removed for confidentiality reasons.

Figure 21 shows the montage of a case study.

This image has been removed for confidentiality reasons.

Figure 21: Electrode montage used in the clinical research in which two electrodes of each type are used to record the brain activity of one hemisphere. The subject is in supine position. (Left hemisphere) Liquid gel electrodes, (Right hemisphere) aCUP-E and (central electrode-reference) aCUP-E. (Case 2).

3.2.5 Skin preparation

Before starting the recording and attaching the electrodes, the neonate's scalp must be prepared. The aim is to remove sweat, grease and dead skin cells that can interfere with the transmission of the electrical activity, increasing the impedance. Also, it is more likely that electrodes attach to a clean scalp.

The process consisted mainly in cleaning the scalp with soap and alcohol, by gently doing circles with cotton swabs. In a few cases, more abrasive methods were used, but there was no evidence of a relevant enhance of the recording. Then the electrodes were attached.

In the commercial case, it is not necessary to add electroconductive gel, as they are already embedded with liquid gel at the factory. Instead, for aCUP-E the gel must be added after placement in the specified hole.

The new electrodes allow easy addition of more electroconductive gel avoiding its drying. So, nurses should add more gel to the aCUP-E every 8 hours. At this step, commercial electrodes should remain untouched since the manufacturer does not ensure a good adhesion after removing them, what would be necessary to add more gel.

3.3 Data acquisition and processing

The *CFM Olympic Brainz Monitor* (Natus Medical Incorporated) has been used to acquire the aEEG signals. The European Data Format (EDF) files containing the raw EEG and the continuous impedances have been extracted from the monitor. There is no option to download the aEEG files in this device.

The signal processing has been mainly performed using *The MathWorks, Inc. (2022) MATLAB,* but the files have been converted to CSV (Comma-Separated Values) using *Python MNE package*, which handled the extracted EDF files better. The files of interest as well as the sampling frequencies are detailed in Table 3.

Moreover, the nurses had some buttons on the monitor's screen to easily indicate events on-board, such as manipulation, cures, electrode replacements… These have been

used to clarify and gain insight about what is happening in specific cases when performing the analysis.

Table 3: Characteristics of the files of interest extracted from the monitor for each acquisition, together with the electrodes (Channels) that record that signal.

File Name	Channel	Sampling frequency (Hz)
LeftEeg	C3-P3 bipolar signal	200
RightEeg	C4-P4 bipolar signal	200
LogicalImpedanceC3	C3 impedance	100
LogicalImpedanceC4	C4 impedance	100
LogicalImpedanceP3	P3 impedance	100
LogicalImpedanceP4	P4 impedance	100

After each recording, the involved nurses filled a survey (part of the research plan) regarding some specific parameters of the case, such as ease of placement and removal, skin safety or subject's specifications. In Annex 1 the survey can be seen, while on following sections these results will be discussed.

3.4 Study population

In the context of this work, the sample was reduced to 15 neonates (11 preterm and 4 term) because at the time this project has finalized the clinical trial was still not completed.

Table 4: Sum up of the subjects of the study. GA = Gestational Age, PCA = Post Conceptional Age at the day of the study , PNA= Post Natal Age at the day of the study. GB = GigaBytes of data.

This table has been removed for confidentiality reasons.

3.5 CFM Olympic Brainz Monitor

The Cerebral Function Monitoring used in this study is the *CFM Olympic Brainz Monitor* from Natus Medical Incorporated (Natus). This business offers medical equipment, software, supplies and services for the diagnosis, monitoring, and treatment of disorders affecting the brain or neural pathways.

This specific monitor (Figure 22) allows recording the raw EEG, the continuous impedance (without stopping the recording) and the aEEG, which is always displayed in the upper part of the screen. Below, the user can easily switch between the raw EEG and the impedance signals by means of an on-screen button.

Figure 22: *CFM Olympic Brainz Monitor* from Natus® [Natus Medical Incorporated. Available at: https://natus.com/products-services/cfm-olympic-brainz-monitor].

While the analog prototype is available, the digital procedures that are used nowadays are not public. This makes it difficult for clinicians and researchers to choose between different brands, because no aEEG standard has been established so far [34]. Figure 23 shows the frequency response curves of different aEEG monitors.

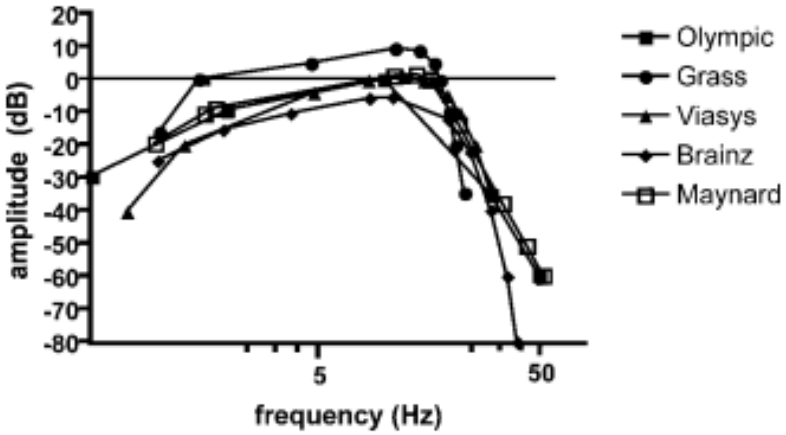

Figure 23:Frequency–response curves from a sample of some digital cerebral function monitors used to generate the aEEG in 2009 [35].

It is likely that companies consider the EEG processing part of their intellectual property (IP) and something with which to put them ahead of their competitors. Therefore, Natus must be using the trade secret strategy, in which valuable information is not known by the public and reasonable efforts are done to keep it secret. Indeed, when contacting with them in order to gain insight about the hardware/software used the answer was *"the requested information is proprietary"*.

Hence, reverse engineering is what has had to be done to understand how the monitor works or how it was made. The aim was to display the same aEEG signal on the computer to be able to work with it, as well as to overcome some limitations found by clinicians.

Figure 24 shows the interface and images that can be extracted from the used monitor.

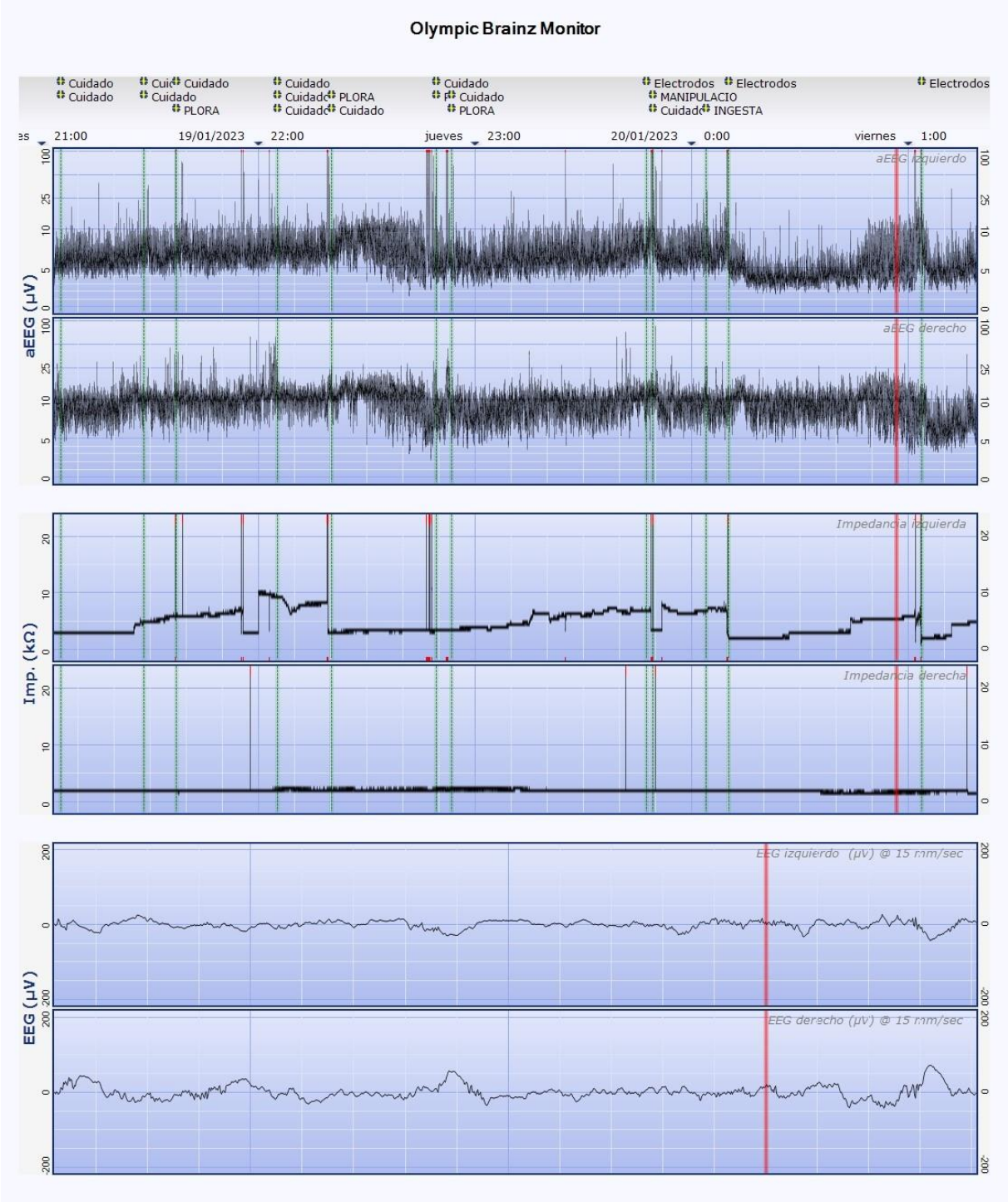

Figure 24: Snapshot of the Olympic Brainz Monitor from Natus. On the very top of the image, the events noted by the healthcare staff. The top section exhibits the aEEG signal (4h 15 mins, starting the 19/01/2023 at 21:00), the middle one shows the impedance maximum from the two electrodes of that hemisphere, and the bottom signal is the 18 second segment of the EEG corresponding to where the red cursor is placed in the sections above. For each of these modules, the upper channel above corresponds to the left hemisphere, while the bottom one is the right hemisphere.

3.5.1 aEEG signal display on a computer

The aim of this section was to be able to evaluate aEEG signals on the computer, and not only be restricted to see and evaluate them in the clinical monitor, which was a drawback of this project. Hence, the accessible and user-friendly interface from the medical equipment should be mimicked, in order to start developing a program that could be used for both, researchers and clinicians. It was thought that developing a User Interface (UI) figure that respected the x-*axis* ratio would be beneficial for the purpose.

3.5.1.1 Digitally obtain the aEEG signal

To replicate the signal that clinicians can see in the *Olympic Brainz Monitor*, the steps described in *2.3.4 Signal Processing* have to be computed, adjusting the parameters to optimize the processing.

When building it, there is three main questions to assess. What filter to use (Figure 23)? How to rectify the signal? How to detect the envelope?

The code of the following sections has been adapted from *Washington University-Neonatal EEG Analysis Toolbox* (WU-NEAT), a clinically validated, open-source *MATLAB* toolbox for limited-channel neonatal EEG analysis [36], and mainly inspired from Zhang D. et al. [30] and Chen C. et al. [29]

To compensate for the skull and scalp attenuation (previously seen in Figure 14), the raw EEG is first passed through an asymmetrical filter which strongly attenuates the signal below 2 Hz (low frequency physiological artifact) and above 15 Hz (respiratory, muscle activity, power line hum …).

The well-known Parks-McClellan algorithm has been used for this purpose, which finds the optimal finite impulse response (FIR) filter coefficients. A high order of 1,100 has been found to perform well, allowing to replicate the signal from the monitor. Other orders were tried, but lower ones failed to follow the aEEG signal from the monitor (next section) while higher orders did not show much improvement regardless the higher computation time (Annex 2). The 12 dB/decade slope in the frequencies of interest is conserved, as well as a strong attenuation in the other bands (Figure 25).

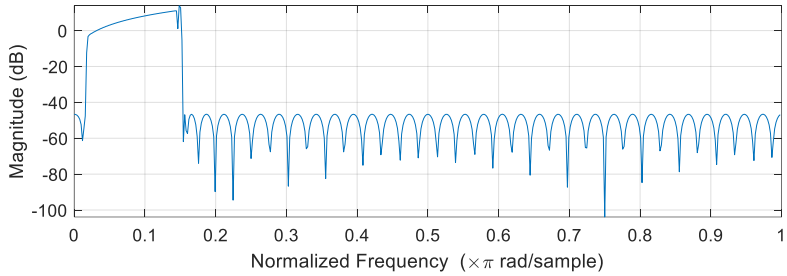

Figure 25: Magnitude of the Designed filter using the Parks-McClellan algorithm with order 1100. Strong attenuation of the <2Hz band, as well as >15 Hz band. 12 dB/decade are approximately conserved between 2-15 Hz. The frequencies on the *axis* are normalized, where 1 corresponds to the Nyquist frequency (fs/2 = 100 Hz).

The filtered signal must be rectified converting the negative values into positive voltages. Digitally, there are two main ways to achieve this: absolute value evaluation or squaring the signal, with a posterior square root of the detected envelope (aEEG). However, not much difference has been detected in the output, and the first option seems to work well for this specific case.

Next, the envelope must be detected, with the aim of getting the amplitude trends of the brain activity. In this work, it is generated by using a Butterworth low pass filter of first order and a strict cut-off frequency of 0.375 Hz (Figure 26).

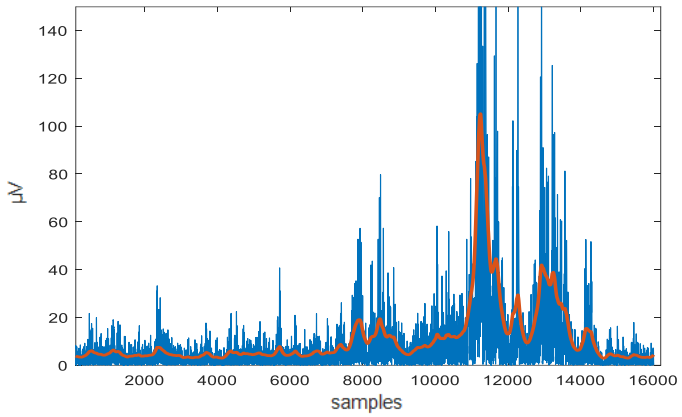

Figure 26: Envelope detection of the signal with a Butterworth filter (fs = 0.375 Hz). The segment is 80 seconds long (16000 samples). Blue: Rectified filtered signal. Red: Envelope or *'raw aEEG'*.

The final step would be to represent the obtained *'raw aEEG'.* It must be represented in a semilogarithmic scale (y-*axis*) and with a ratio of 6 cm/hour for the x-*axis*.

In the program, the y scale is achieved by performing the logarithm with base 10 to the voltages above 10 μV, obtaining a semilogarithmic voltage. Then, *y ticks* are changed to display them in accordance with the graph. Moreover, the dimensions of the window have been settled to respect the x-*axis* ratio (25.5 cm for 4 h and 15 min, which equals 6cm/hour).

3.5.1.2 Comparison of the obtained signal

The monitor used doesn't have the option to extract the aEEG signal in any format, only the raw EEG. Hence, there is no way to statistically compare both data (e.g. Spearman Rank Correlation) and a visual assessment must be performed. In Figure 27 the computed signal is represented in blue, superimposed to an image from the monitor. In Figure 28, a different segment is shown without overlapping.

With the constructed algorithm, the obtained signals are almost identical to what can be seen in the screen of the monitor, reinforcing its validity. Annex 2 shows the fitting of signals built with different filter orders.

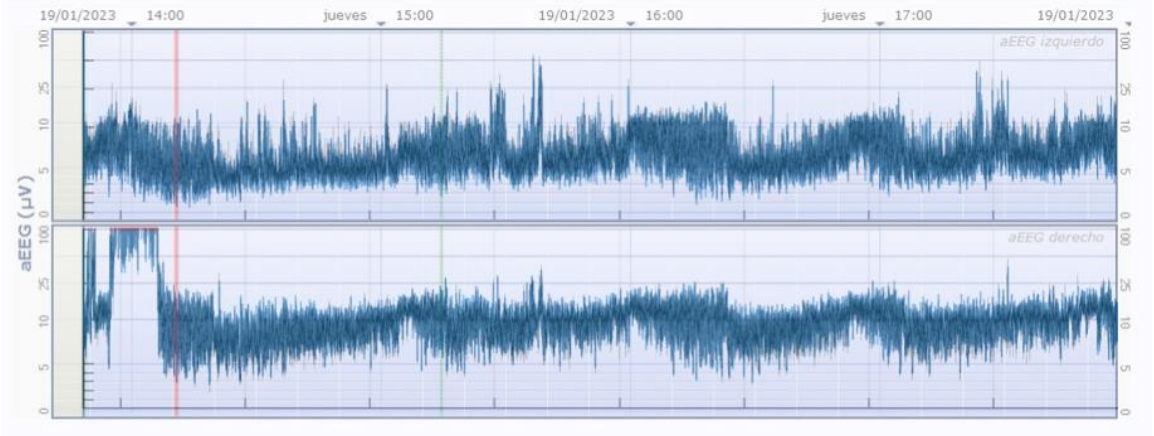

Figure 27: Case 3 (19/01/2023). Blue: aEEG built signal. Background: Image from *CFM Olympic Brainz Monitor*, Natus.

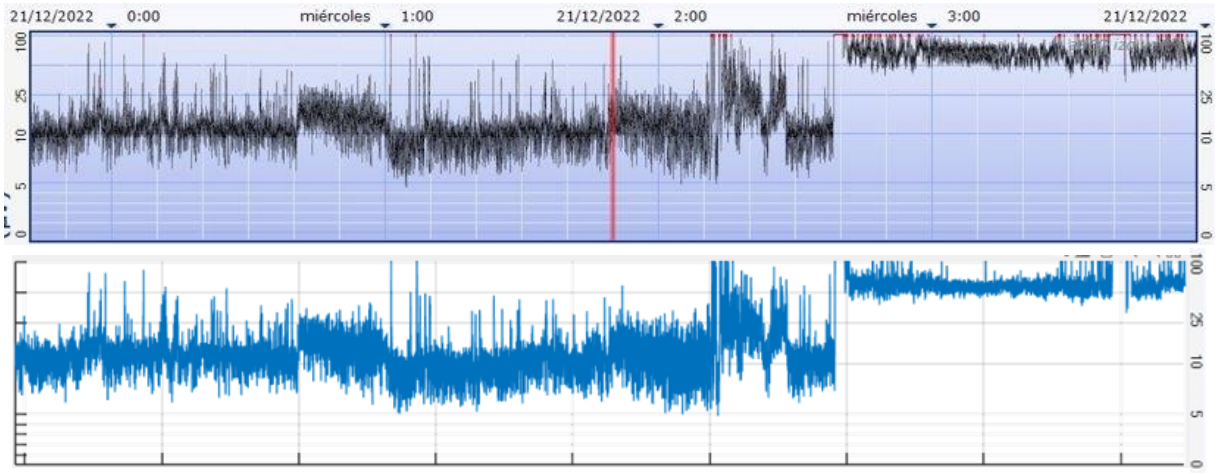

Figure 28: Case 1 (20/12/2022). Fragment of aEEG recording. (Above) Signal from the *CFM Olympic Brainz Monitor*, (Bottom) Digitally obtained signal.

3.5.1.3 User Interface

The aim of this approach is to mimic the used aEEG monitor on a computer. Then, users must be able to evaluate both hemispheres at the same time and should have same characteristics as the medical monitor. Moreover, the variables are saved in the workspace for further mathematical analysis. The code to reproduce this interface can be seen in Annex 3.

As the x-*axis* ratio is settled and the screen size is limited, not the whole recording can be seen at once. Because of this reason, a slider is used to allow the user to navigate and explore different time segments, always conserving the 6 cm/h.

The upper and lower margins of the aEEG seem to be of big importance to take clinical decisions, and it is a differential feature for some classification analysis of the aEEG (Burdjalov or Hellstrom-Welltas). These envelopes allow to clearly see the brain activity tendencies and differentiate between different phases and states. Since the aEEG signal is compressed in time, to detect the envelope the data is largely downsampled, keeping the 97^{th} and 6^{th} percentile (upper and lower margin respectively) from epochs of 8 seconds. Finally, the median amplitude of 20 consecutive points, previously computed (8 seconds/point * 20 points = 2 min and 40 s) is again performed to obtain a smooth representative margin [30]. These edges can't be seen in the used monitor. Since it is a plus, there is a button on the UI to enable this feature or not (Figure 29).

Finally, the detection of electrical activity not coming from the brain has also been computed, indicating to the observer which time segments contain non-optimal electrical activity (contaminated) by electromagnetic interferences (EMIs), moving artifacts or impedance instability. There are many artifact detection and recognition algorithms focused on adult multichannel EEG, but none are focused on neonatal aEEG. Therefore, the aim would be to compute a first approach to allow the observer to identify regions of optimal brain activity to be more accurate in the diagnosis, as well as to be able to restrict the signal analysis to regions of interest.

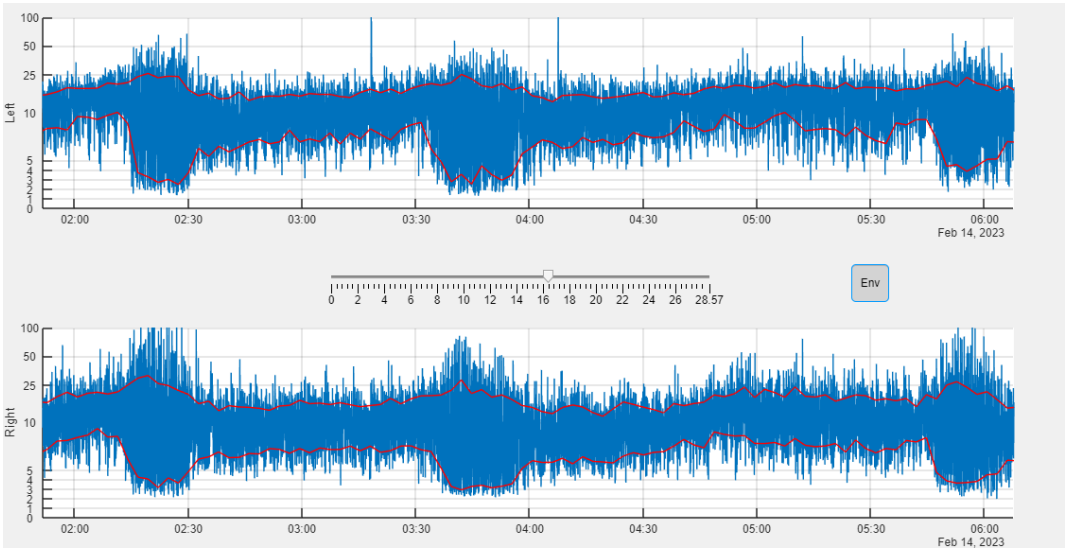

Figure 29: User Interface with the built aEEG signals. Both hemispheres can be seen, as well as the computed margins. Button Env. allows displaying or not the margins, while the slider moves and navigate through the signal (Case 2).

To achieve this objective, we have worked hand by hand with Dr. Vicenç Pascual, who first posed the problem and visually validated that the algorithm detected the appropriate fragments. Two restrictive neurophysiologic parameters were defined to characterize waves not coming from the brain.

1. EEG waves of more than 150 μV and of more than 2 seconds long are unlikely to come from brain activity (Figure 30).
2. Low aEEG peak-to-peak amplitudes are due to other factors rather than brain activity(Figure 31).

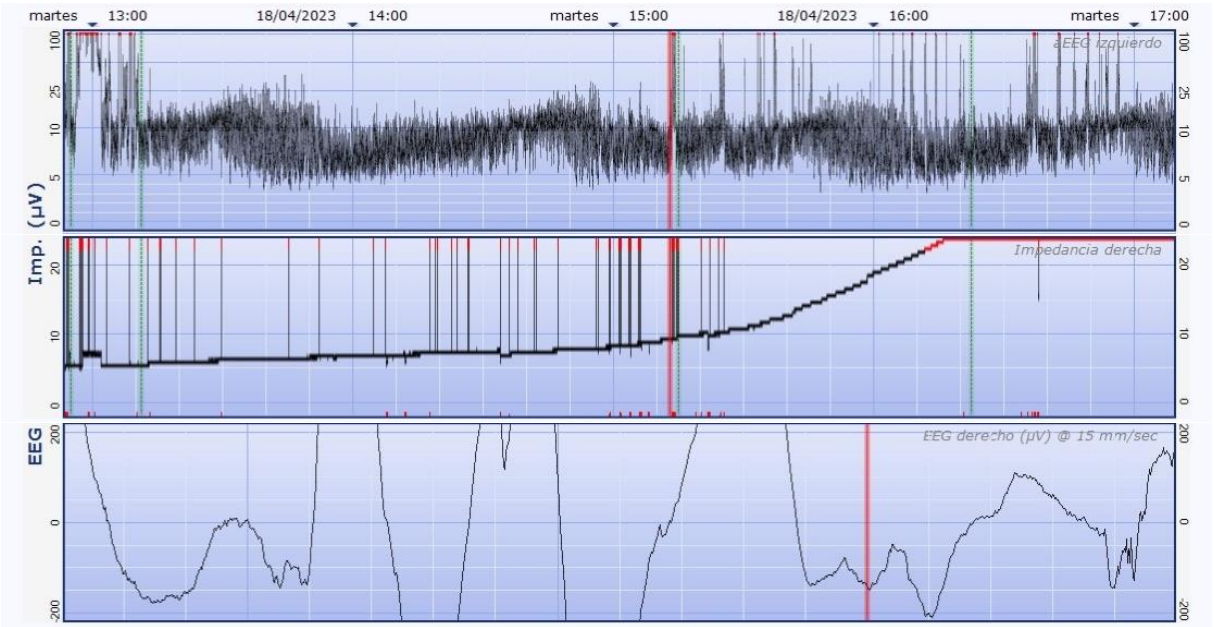

Figure 30: 1st restriction, in which high amplitude waves more than 2 seconds long can be seen in the EEG. In this case, the abnormal activity recorded is due to impedance variations. (Top) aEEG with the timescale on the top. The red cursor restricts the area of the EEG. (Middle) Impedances, with same x-*axis* scale as the aEEG. (Bottom) The EEG belonging to the 18s indicated by the previous red cursor, each vertical white line corresponds to a second. (Case 11)

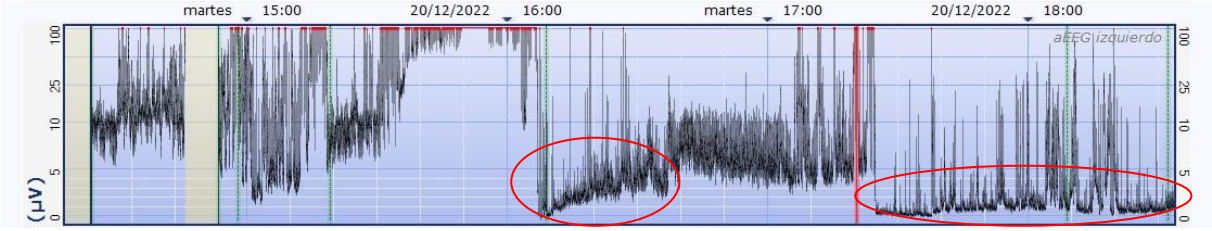

Figure 31: 2nd restriction, in which the aEEG presents narrow bands (red line). Rather than brain activity, this is attributed to a conductive bridge between the electrodes of the same hemisphere, obtaining the same input. (Case 1)

Therefore, the non-cerebral activity is going to be filtered out in the aEEG processing. However, since the first condition is based on the raw EEG, there is the possibility, that it has no big effects on the displayed aEEG signal. But the aim is to quantify the number of artifacts detected that can potentially interfere with the processed aEEG, warning the observers about it, but leaving it to their own judgment. Also, some artifacts may be leaked because they are confounded with brain activity that comes from the brain (don't meet the restrictions), so critical knowledge is still needed.

The steps followed to achieve the identification of non-cerebral activity are detailed next:

- For the first condition:

1. Detect the points that are above 150 µV in the raw EEG.
2. Focusing on just one point, get a 18s segment (like the monitor) around it.
3. Smooth the signal (symmetric moving average) to be able to detect the peaks of interest, not the small signal variations. Correct the filter delay. Any symmetric filter of length N has a delay of (N-1)/2 samples. (Figure 32).
4. Check if within this segment there are any peaks (maximums or minimums), that are at least 2 s apart.
5. Now, it must be checked that the two features relate to the same wave. Since some amplitude resolution is lost with the moving average, we check if the first condition is fulfilled within the original signal.
6. If step 5 is true, reject the whole 18s segment because it is affected, and such a little time won't have any effect on the aEEG time compressed visualization.

- Check for the second condition using the margins. If the width is lower than the threshold (2 µV), reject the segment around the margin point (1 min and 20 second to each side, half of the sampling period of the margins).

Finally, everything is integrated into the UI which has allowed seeing the recordings in the computer as well as evaluate some differences and characteristics. Since the optimal brain activity is also a plus, there is a button to enable this feature were green means optimal and red means non-optimal. Figure 33 shows the final interface in segment in which the left hemisphere was not properly recording due to a detached electrode that had to be replaced later on. For the right hemisphere, the patterns are detected with some artifact.

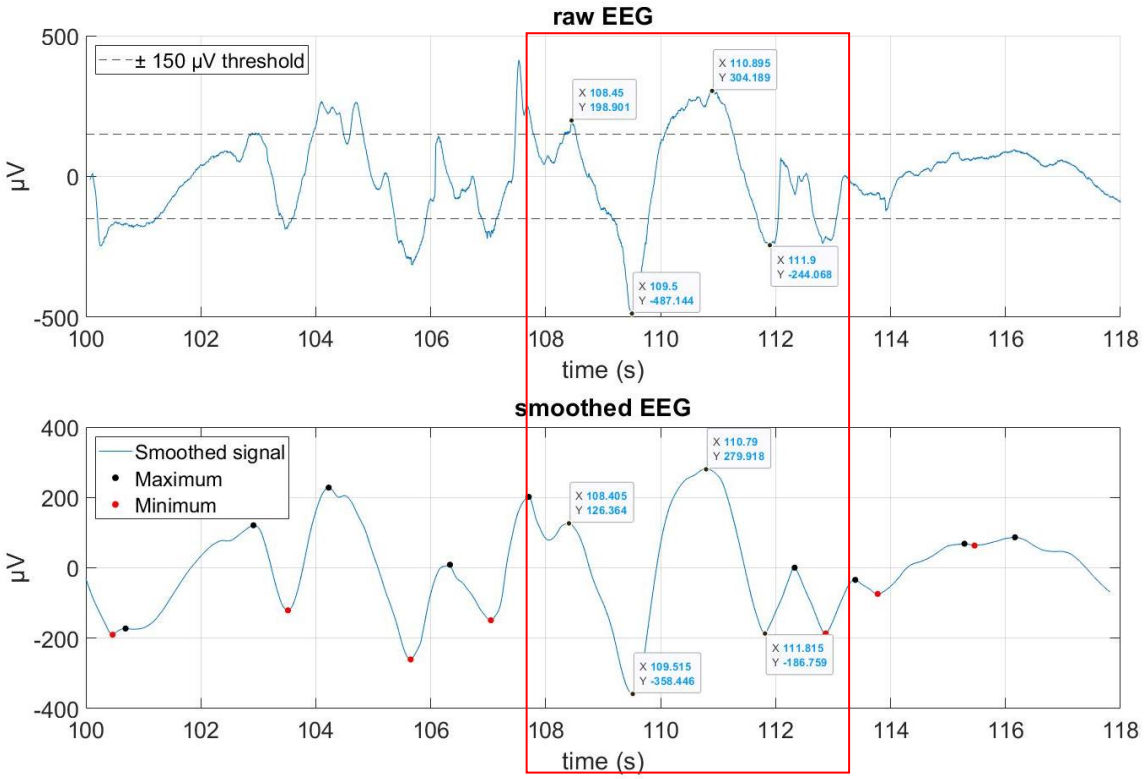

Figure 32: Peak detection to assess non-cerebral electrical activity. The smoothing corresponds to a moving average, which changes the amplitude resolution. Red square indicates a region of abnormal activity, where peaks are separated more than 2s and higher than the threshold (18 seconds extract of Case 1)

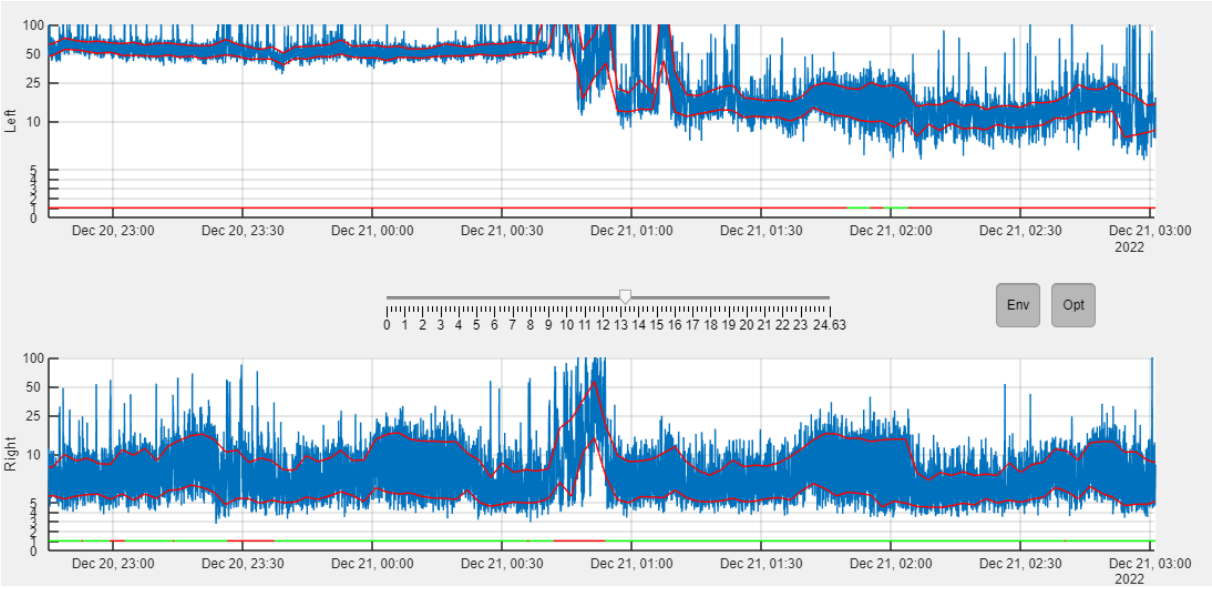

Figure 33: UI program built in *MATLAB*, simulating an aEEG monitor. The aEEG (blue), the envelope (red line) and the parts where non-cerebral brain activity has been detected (straight line at the bottom of each hemisphere. Green: Cerebral activity, Red: Artifacts detected) can been seen. The signal in the top is the left hemisphere, while the one in the bottom is the right hemisphere (Case1). Button *Env* enables the margins while *Opt* enables the optimal/non-optimal line.

3.6 Methodology for the analysis

The aEEG signal created in the previous section, together with the impedance values and the raw EEG, permitted to focus on an analysis, which is detailed in this chapter.

3.6.1 Parameters

Different parameters have been computed to try to characterize some features of the recordings and be able to compare both electrodes, aCUP-E and Neuroline 720. Signal quality, electrode life, impedance stability among others.

To reduce the artifacts and obtain the signal, Independent Component Analysis (ICA) techniques are widely used in EEG, obtaining results from brain activity signal, location, and interferences [37], [38] . Due to the limited number of channels in aEEG, this technique cannot be used.

In the analysis, some characteristics are time dependent. In this cases, same-time different location approach has been used, in which comparisons between hemispheres (different location) are made within the same time frame of the recording. This allows to avoid inter-patient differences due to electrode positioning or attachment [39].

For frequency domain features, the raw EEG is the subject of study. Frequential components of interest, together with noise are quantified for different epochs before the aEEG filtering. The aim would be to characterize the signal-to-noise ratio (SNR) of each electrode. Higher and more stable SNR would allow for a more accurate postprocessing [39], [40].

Regarding impedance features, the $k\Omega$ extracted from the monitor for each channel are used. It is known that when lower and more stable, the better the recording [35], [40].

The code with the functions used to obtain these features can be found in Annex 3.

3.6.1.1 Interhemispheric signal comparison

In this section, the aim is to delve into a comprehensive analysis of the brain activity dynamics between the two hemispheres, aiming to test a specific hypothesis that will let us use the data for further investigation.

The neonates brain activity should be alike in both hemispheres for healthy subjects due to the symmetrical development of the neuronal population. This interhemispheric comparison is crucial to test this hypothesis and make sure that both electrodes capture the same signal when optimally recording. As a result, the following signal differences could be attributed to electrode design [14].

To do this, the recordings of the clinical trial must be filtered. Hence, 2 parameters have been defined to assess how representative or useful they are. Even so, these 2 variables also help to gain insight into the data.

3.6.1.1.1 Optimal brain activity

To compare interhemispheric electrode capture, we must ensure that we are comparing a time frame in which both electrodes are capturing the signal without artifacts and, guarantee that the impedances are low and stable. If not, the differences found in the aEEG signal may be due to these defects.

Therefore, this parameter is based on the previously detected optimal brain activity in order to see how both electrodes capture the signal and, assess if there is enough time (at least 2 hours) in which both hemispheres have optimally recorded. If this last requirement is

not fulfilled, these recordings won't be selected for further signal analysis, since there won't be enough time to perform the following amplitude analysis (same-time different location).

Two hours of good recording in both hemispheres has been considered to be representative enough to evaluate at least one sleep-wake cycle (Figure 34), which is the expected pattern in our population (healthy neonates). With this, all the amplitude features as well as all the frequential components that can differ from vigil/REM sleep (narrow) and no REM sleep (wide) can be assessed.

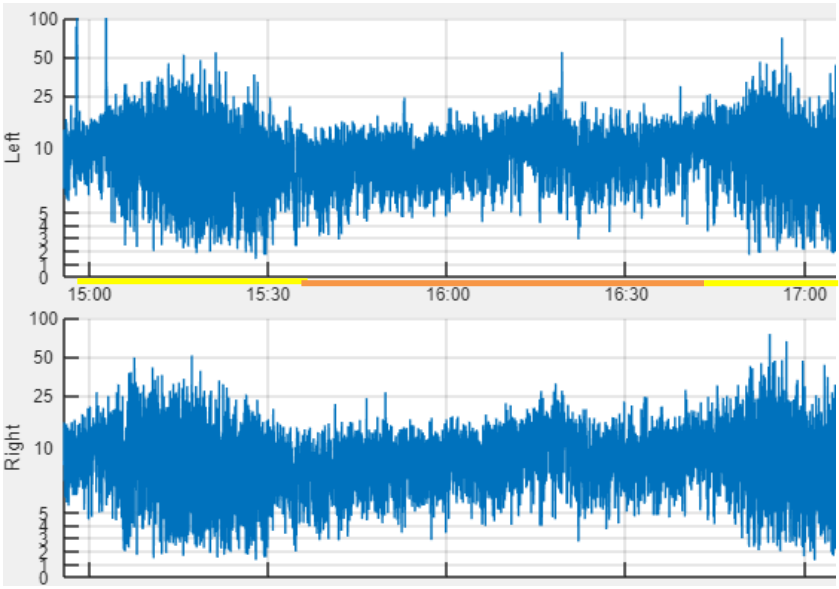

Figure 34: 2 hours segment. REM / vigil (narrow, orange) and no REM sleep (wide, yellow) segments can be seen and assessed this time. (Case 3)

3.6.1.1.2 Amplitude features

Separately positioned electrodes record different bioelectrical activities, while closely located capture more similar signals coming from the brain (even there is the possibility of causing a conductive bridge). This positioning has an effect in the amplitude of the bipolar signal, which is built with a differential amplifier. Hence, electrode location is a crucial factor in aEEG [39].

Several studies comparing wet and dry electrodes assess the resemblance of the captured signal in a near position (within 10 mm) of an adult EEG [39], [41]. In the aEEG montage used, the electrodes are not closely positioned. However, both hemispheres should develop at the same time (same brain activity) in healthy neonates [14]. If during optimal impedance times significant differences in aEEG amplitude are found between the signal captured in both hemispheres, these should be attributed to the placement of the electrodes. In these cases, comparing the two hemispheres would not be relevant in terms of signal analysis.

Therefore, to avoid other interferences, this hypothesis is tested in the previously computed 2 hours segment with optimal brain activity, together with low (ideally <5 $k\Omega$) and stable impedance for the four electrodes. These 2 conditions are usually simultaneous and allow to evaluate the amplitudes of a whole sleep-wake cycle. It would be expected to see a similarity between both hemispheres, since ideal conditions are selected and there should be no distortions.

To perform this analysis, from the obtained segments, the Root Mean Square Deviation (RMSD), the maximum and minimum, as well as the correlation (Pearson Correlation Coefficient) of the margins has been computed to evaluate the interhemispheric signal

similarity in a time-domain analysis. The first one, assesses the direct differences between the signal, the second assesses the extreme values of the margins of both hemispheres, while the latter evaluates the brain activity tendencies in both hemispheres.

This analysis will be used to check if the two hemispheres resemble each other in optimal conditions for each case and, therefore, the found differences in other signal segments can be attributed to the electrodes design rather than the montage. Different width of the trace, which is related to the peak to peak amplitude, can lead into differences in signal power even if the trace is correlated (similar brain activity tendencies).

3.6.1.2 Preliminary assessment

In this section, we embark on a comprehensive evaluation of the recorded data, aiming to assess the fundamental characteristics of the acquired signals before entering an in-depth analysis. Some characteristics of each record are assessed in order to have an overview of how they have gone, and which factors make them behave like that. Recognizable frequential components and impedances are assessed.

3.6.1.2.1 Impedance summary

Each hemisphere has two impedance values, one for each of the four recording electrodes (not the reference). In order to simplify the data into just one representative value for each hemisphere, the same criteria as the monitor (*CFM Olympic Brainz Monitor*) is used: The maximum between the two impedances of each hemisphere is computed over time. This ensures that both electrodes of the same type (one hemisphere) are under the defined thresholds on a specific moment.

Within this section the aim is to visually assess the quality of the adhesion and gel drying (impedances) in the recording. To do so, two main parameters are computed.

Firstly, the percentage of time that the two electrodes of the hemisphere have been between certain thresholds. The bands are: *≤5 kΩ, >5 & ≤10 kΩ, >10 & ≤15 kΩ, >15 & ≤20 kΩ, >20 kΩ.* A traffic light colour palette has been used to easily identify which records have had a better impedance value and compare between hemispheres.

Secondly, turns count, which consists in recording the number of times a signal is above a certain threshold [42], is computed. In this sense, the rising edges were detected in the cases that the maximum impedance of each hemisphere exceeded 20 $k\Omega$. The time that the impedances stayed above the threshold was also calculated. The results are presented normalized by the length of the recording in hours (counts/hour).

This parameter has been displayed in 3 graphs of interest. The amount of variability of the impedance (turns count lower than 10 seconds), which can lead to misinterpretations of the aEEG signal and is highly related to the quality of the adhesion. More impedance spikes mean that the electrode adhesion was poor and more susceptible to cable movement artifacts. If these impedance oscillations last longer they may produce an increase on the aEEG voltage, which can be confused with a neonatal seizure (10 s to 1–2 min), being more critical for the diagnosis. To have this effect, the spikes do not necessarily have to overcome the set threshold. However, little to none of the variations remain lower than 20 $k\Omega$ because they are usually related to an act that totally cancels the contact between the electrode and the scalp. So, this limit is kept.

Also, the number of times that the electrode ceased to function well for a long time (>20 $k\Omega$ for more than 30 mins) for each hemisphere. The latter is also a clinical concern because not recording the signal may hinder the fast diagnosis of neonates.

3.6.1.2.2 Frequential domain summary

A Fast Fourier Transform (FFT) is a mathematical technique that allows to analyse signals and understand their frequential components. It's a powerful tool that converts complex signals into individual frequencies.

This method is widely used for the characterisation of EEG signals and feature extraction [40], [43]. In this work, it is computed for each record, to evaluate the frequency domain of the signal. The aim is to see frequential components of interest in the neonatal bipolar raw EEG, as well as assess if there is any strange frequency in some of the cases, which may be due to the brain activity (no problem) or to the electrically hostile environment of the NICU (influencing the signal).

Ideally, electromagnetic interferences (EMIs) should not have any effect because of the nature of the instrumentation amplifier, that cancels out same input's voltages in both entries. However, the antenna-like behaviour of the electrodes opposes to it.

Three different FFT are computed to completely evaluate the spectrum:

- The entire recording: Overall assessment of the adherence by the voltage of the 50 Hz noise [41].
- Notch filtering the 50 Hz noise: Evaluate other frequencies that appear in the whole recording, that were before hidden by the electric hum [44].
- 2 hours of optimal brain activity together with low (ideally < 5 $k\Omega$) and stable impedance is for the four electrodes: The aim is to differentiate between the frequencies that appear in the whole recording, but do not appear when the impedance is optimal. These different amplitude voltages, that may be due to impedance influence, are candidates to induce artifacts. Recordings in which these conditions are not able (not selected), won't display this last graph.

3.6.1.3 Survival analysis (Electrode life)

The time in which each electrode stopped working was computed thanks to the impedance continuous monitoring that the monitor provides. In this sense, a cease of the functioning (detachment or gel drying) is considered when an electrode exceeds 20 $k\Omega$ for at least 15 minutes, which is more than the average time that it takes for the nurses to provide the care (assessed in the monitor annotations). When this impedance lowers, it is considered that the electrode has been manipulated/replaced and the count is restarted for this new electrode.

Another assumption is that based on the analysis that *El Ters et al.* [33] conducted on electrode survival, all of them are considered to last at least 45 minutes. Detachments before this time will be considered as a *procedure error* when adhering them to the scalp and won't be considered for the analysis. These 2 assumptions will be used to build the algorithm.

Kaplan-Meier curves have been used to estimate the survival function and allows accounting for censored data [45]. In this analysis, only the first 24 hours have been considered, because having recordings of different lengths affected the approximation of probability function. Hence, all records will be trimmed. If after 24 hours the electrode is not deteriorated, the time since its last replacement will be right censored.

Censoring means that the measurement is only partially known. Hence, the previous case is considered as if *'the track of the electrode was lost'*. Since the algorithm detects the events, there is certainty about it (exact time of failure is known), therefore, they are not left censored[45]. Figure 35 shows a scheme of the censorship.

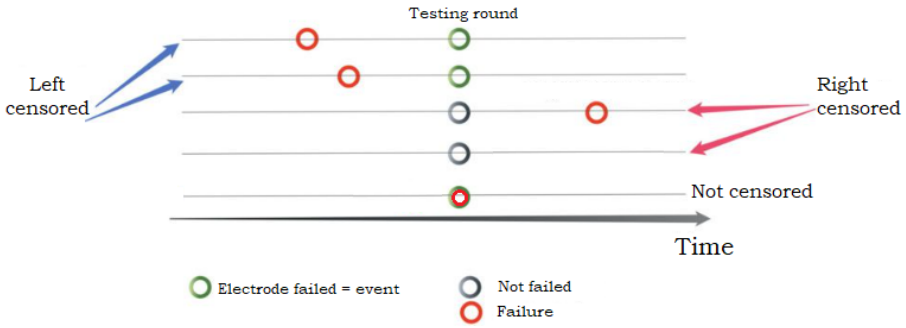

Figure 35: Example of tests, where the testing is performed at a discrete time. Two left censored, two right censored and one non-censored. No censorship means that the exact time of failure is known, left censorship means at that time it had already failed, right censorship means at that time it has still not failed. Modified from: [46].

3.6.1.4 Impedance stability

The variability of the impedance along the recording is an important factor. What's more, it may be even more crucial than its actual value ($k\Omega$). Figure 36 shows a segment of a high but 'stable' impedance recording in which the acquired signal is good. It can harden the diagnosis, but there are still some recognizable patterns and a decent raw EEG. Indeed, unfirm impedances (marked in red) is what induces the variabilities in the signal detected by the electrode, which are not due to the brain activity. Hence it can simulate an epilepsy and cause a clinical error.

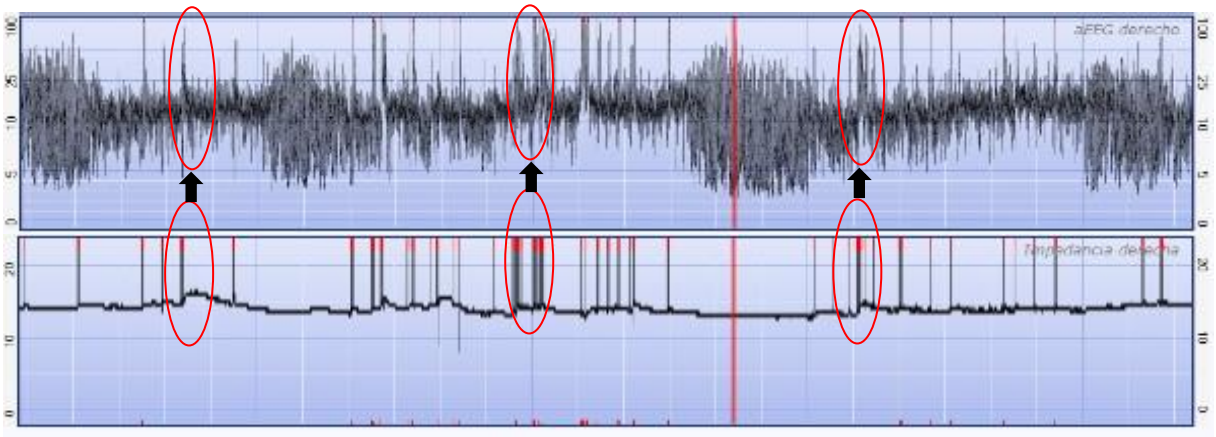

Figure 36: High impedance recording of the right hemisphere, in which a high but stable impedance (>10 $k\Omega$) is seen in the segment, but still recognizable patterns (aEEG) and a decent EEG signal can be seen. Red circles show the effect of an impedance spike, which leads to an increase of the aEEG voltage.(Top) aEEG, (Bottom) Impedance. (Case 9)

To characterize this variability, a moving standard deviation has been computed for each electrode of each recording [42]. Thirty minutes segments have been taken, with an overlap of 50%. From the obtained value (SD) for the segments of each recording, the mean as well as the standard deviation will be computed, to assess any statistical difference.

3.6.1.5 Susceptibility to different frequency ranges

As a general rule, the power around the line noise frequency tends to increase with increasing electrode impedance values. Several research has been conducted in order to compare the impact of 50 Hz noise power across different impedance ranges [41]. By

leveraging the continuous monitoring capabilities offered by the device employed in this research, an in-depth investigation can be conducted to explore the susceptibility of various frequency ranges within more specific impedance values. The primary goal of this experiment is to see if both electrodes behave similarly when examining the frequency components collected by them.

This analysis is performed in the framework of aEEG, hence the frequencies between 2 and 15 Hz will be considered the signal. For the noise, there is more controversy. Its proper definition would be: *Any unwanted signal, random or deterministic.* This is a not very specific, since in EEG signals, we have two sources of noise. The first one is the natural physiological noises such as breathing, cardiac pulse, muscle contraction… The second is the noise that comes from outside of the brain, which is the one of clinical concern.

However, in this specific case there are some frequency bands that are of more interest than others:

- 0-2 Hz: Should be no difference between electrodes when there is a good impedance, both would capture. (Physiological artifact).
- 15-46 Hz: May be some difference between electrodes, due to the movements related to these artifacts. (Respiratory and Muscle activity).
- 50 Hz: Mains Hum Noise. Less noise is going to be captured with a good electrode performance.
- 51-100 Hz: There is little probability to have physiological artifacts of this frequencies.

The power of the different frequency bands for the different segments will be characterized in order to assess any significant differences in the recording.

The intention would be to compare the frequency components that appear in small time frames that allow to not consider impedance variability. In this sense, one-minute fragments seem to be a good trade-off between enough frequency resolution and little time to neglect the changes that impedance variability induces on the signal. However, this, together with the electrode positioning and the changes in brain activity will induce some variance in the results.

This analysis will shed light on the extent to which electrode impedance affects the evaluation of frequential components.

3.6.1.6 Signal quality

Signal quality is also a feature widely studied for EEG characterisation, but that has had to adapt to this work. Usually, the Signal to Noise Ratio is computed on short segments of interest where de adult is performing a specific task, not on long recordings such as the ones on this clinical trial [47].

To be able to assess the signal quality within the same recording, several fragments have to be extracted. The aim is to compare which type of electrodes had a better signal quality for that specific recording. In this sense, it can be evaluated if the improvements of aCUP-E actually translate in a better signal acquisition. To avoid considering whole recordings with all the assumptions that this entails, we'll focus the signal quality analysis only to fragments in which none of the electrodes is detached. The signal will be split in one minute segments, as defined in the previous section.

It must be contemplated that when detached, an electrode has an antenna-like behaviour, amplifying different EMI's. This may influence the capture of the signal or the SNR. Hence, the 50 Hz noise is going to be used as an 'approximation' of the capture of noise from outside of the brain.

Equation *(2)* describes the computed signal to noise ratio in dB, from which the power of the frequency bands has been obtained using *pspectrum* function.

$$\mathrm{SNR} = 10 * \log_{10}\left(\frac{Signal\ Power\ (\mu V^2)}{Noise_{50Hz}\ Power\ (\mu V^2)}\right) \quad (dB) \tag{2}$$

3.6.2 Statistical analysis

To compare and characterize the difference between hemispheres for each subject (impedance stability and signal quality), a statistical test has to be performed to evaluate if the variations are significant. Since normality is not achieved in most of the data collected (condition of *T-student* test) because of fluctuations along the recording due to different factors. Hence, the non-parametric Mann-Whitney U test has been used for this purpose. Nevertheless, the statistical tests have also been computed using T-Student to assess any major difference.

The test has been performed one sided, in which the alternative hypothesis is that aCUP-E performs better (higher or lower depending on the case), not just assessing the differences. The equations *(3)*, are the null (H_0) and alternative hypothesis (H_A) of the different cases. In the Mann-Whitney U test, M corresponds to the median of each statistical population: aCUP-E or Commercial data.

$$H_0: M_{aCUP} - M_{Commercial} = 0 \tag{3}$$
$$H_A: M_{aCUP} - M_{Commercial} > 0\ or\ M_{aCUP} - M_{Commercial} < 0\ 0$$

The result of the tests is a p-value (p_{val}), which indicates the significance level of the obtained result, which allow us to reject the null hypothesis with a certain confidence. Since we are performing a clinical investigation, a $p_{val} \leq 0.05 = \alpha$ is used to indicate statistical significance.

In the sections in which comparisons are made for each subject, a Bonferroni correction is then performed. The objective is to avoid type I error in which something is selected significant while it is not [37]. As an example, if $\alpha = 0.05$ and the test is performed for 20 different cases, $20 * 0.05 = 1$, it should be expected to wrongly analyse one case. This multiple test problem scales as more analysis are performed. Hence, to avoid further statistical errors:

$$\frac{\alpha}{nº\ of\ tests} = \frac{0.5}{15} = 0.033 = \alpha_{Bon} \tag{4}$$

When assessing electrode survival, a log rank test has been used to test the null hypothesis that there is no difference between the two electrodes to observe an event (cease of functioning) at any time. All calculations should have the same weight, using Tarone-Ware test for this purpose $(p_{val} < \alpha)$ [33].

For the susceptibility, since there is enough resolution for the two axes, a curve fitting relating the SNR in logarithmic scale (dB) and the impedance in $k\Omega$ (imp) will be performed for each electrode ($f(imp) = SNR$, where f is the regression). In order to select the most appropriate method two parameters describing the goodness of the fit will be evaluated. In this case, adjusted R-square (Equation *(5)*) and Root Mean Square Error (RMSE) are used.

$$\mathrm{R}^2\mathrm{Adjusted} = 1 - \frac{(1-R^2)(N-1)}{N-p-1}, \quad (5)$$

where $p = nº\ of\ predictors,\ N = sample\ size$ and $\mathrm{R}^2 = 1 - \frac{\sum(y_i - \hat{y}_i)^2}{\sum(y_i - \bar{y})}$;

where $\hat{y}_i = predicted\ y\ value$ and $\bar{y} = mean\ of\ y\ values$

4 Results and discussion

This section has been removed for confidentiality reasons.

4.1 Recordings overview

4.2 Interhemispheric signal comparison

4.2.1 Optimal brain activity

Table 5: Sum up of the different percentages of the recording in which optimal a non-optimal electrical activity has been detected. Longest segment in hours.

Figure 37: Summary of the optimal brain activity captured for each electrode along the different cases. (Purple) Commercial electrodes, (Orange) aCUP-E, (Grey) Both electrode optimally recording simultaneously.

4.2.2 Amplitude analysis

Table 6: RMSD of the two hours segment. Max, min and correlation analysis (Pearson Coefficient) of the upper and lower margin in 2h segments.

Figure 38: 2 h optimal segments (green line at the bottom) for the first 5 recordings, in which the same tendencies can be seen in both hemispheres. (Top) Left hemisphere, (Bottom) Right hemisphere.

4.3 Preliminary assessment

4.3.1 Impedance

4.3.1.1.1 Impedances percentage

Figure 39: *Traffic light* graph summarizing the percentage of time that both electrodes of each hemisphere have been under a certain impedance threshold.

4.3.1.2 Turns count of impedance values over 20 $k\Omega$

Figure 40: Turns Count of fast impedance oscillations, remaining less than 10 seconds over 20 $k\Omega$.

Figure 41: Turns Count of Impedance oscillations (over 20 $k\Omega$) lasting the same as the average Neonatal Seizure time

Figure 42: Turns Count of Impedance oscillations (over 20 $k\Omega$) lasting more than 30 minutes, which can be related to deadhesion.

4.3.2 Frequential domain

Figure 43: Case 1 Fourier transforms. (Top) Commercial electrodes, (Bottom) aCUP-E. (Left) FFT of the entire recording, (Middle) FFT of the entire EEG with Notch filtering the 50 Hz noise, (Right) Transform of 2 hour of ideal recording in which the impedance is under 5 $k\Omega$ for the four electrodes.

Table 7: Sum up of the observations seen in the different cases in which that specific hemisphere (electrode type) has had a higher frequential component. The *Higher 50 Hz noise* as well as *Higher Signal* are obtained from the entire recording.

4.4 Survival analysis

4.4.1 Entire clinical trial

Figure 44: Plot for longevity curves of each electrode type, no matter their position. (Tarone-Ware: $X =$, $p_{val} =$)

Figure 45: Plot for longevity curves for each electrode type. (Left) Electrodes on the central (C3-C4) positions (Tarone-Ware: $X =$, $p_{val} =$), (Right) Electrodes on the parietal (P3-P4) positions (Tarone-Ware: $X =$, $p_{val} =$)

4.4.2 Refined data

Figure 46: Corrected survival analysis (Kaplan-Meier curve) in which manipulations and breaches of the protocol are not considered as a cease of the functioning. (Tarone-Ware: $X = 11.38$, $p_{val} = 7.42e-4$)

Figure 47: Corrected survival analysis (Kaplan-Meier curve) in which manipulations and breaches of the protocol are not considered as a cease of the functioning. (Left) Electrodes on the central (C3-C4) positions (Tarone-Ware: $X =$, $p_{val} =$), (Right) Electrodes on the parietal (P3-P4) positions (Tarone-Ware: $X =$, $p_{val} =$))

4.4.3 Only first failure

Figure 48: Corrected survival analysis (Kaplan-Meier curve) only considering the first detachments. (Tarone-Ware: $X =$, $p_{val} =$)

Figure 49: Corrected survival analysis (Kaplan-Meier curve) only considering the first detachments. (Left) Electrodes on the central position (Tarone-Ware: $X =$, $p_{val} =$), (Right) Electrodes on the parietal position (Tarone-Ware: $X =$, $p_{val} =$).

4.5 Impedance stability

Figure 50: Example of case 7 impedance for the different positions (left) as well as for the different electrodes (right). Red points are outliers.

Table 8: Moving Standard Deviation results. Segments of 30 minutes with 50% overlap. The mean and SD sum up the distribution of the computed SDs for each recording.

Figure 51: Average of the standard deviation of each segment for each record. impedance variability among segments (SD) of each recording. (Left) Mean variability value of each electrode type and position for every recording, (Right) Variability value of each electrode type (mean between locations) for every recording. Red points are outliers while black diamonds are the mean for all the patients.

4.6 Susceptibility to different frequency ranges

Figure 52: Signal (dBµV) captured for aCUP-E (left) and commercial (right) electrodes at different impedance ($k\Omega$) values.

Figure 53: 50 Hz noise (dBµV) captured for aCUP-E (left) and commercial (right) electrodes at different impedance ($k\Omega$) levels.

Figure 54: Signal to Noise Ratio (SNR) captured for aCUP-E (left) and commercial (right) electrodes in dB at different impedances ($k\Omega$). Black dashed line represents the regression line (2nd order polynomial) from the data, which estimates the natural behaviour of the electrode.

Table 9: Different types of curve fitting for the aCUP-E and Commercial SNR depending on the impedance. R^2= Coefficient of determination, RMSE= Root Mean Square error. For the equations: a,b,c,d = coefficients of the regressions, x = impedance in $k\Omega$, y = SNR in dB.

Figure 55: Regression Lines with its equations and coefficients. Colour code is respected, being orange aCUP-E and purple commercial. (Top left) 2nd order polynomial, (Top right) Power equation, (Bottom) Sum of two exponentials

4.7 Signal quality

Table 10: Signal to Noise Ratio (dB) of 4 recordings. Segments of 1 minute for each recording are evaluated to compute the statistics.

Figure 56: Extract of the recording of Case 1 of a decent segment for both hemispheres. However, aCUP-E (right) has a cleaner trace, in which brain activity can be better observed. On the other hand, commercial electrodes show more susceptibility to artifacts (spikes) hardening the evaluation of the brain activity tendencies and patterns.

4.8 Opinion Survey

4.8.1 Ease of electrode placement and removal

Figure 57: Results of the ease of electrode placement survey answered after each recording.

4.8.2 Skin safety

Figure 58: Results of the skin safety survey answered after each recording.

5 Conclusions

The results of the present study show that aCUP-E electrodes exhibit better adhesion and higher impedance stability than the ones used nowadays in clinical practice. This translates into a better signal quality of the recordings together with an enhanced electrode life, which results into a better interpretation of the aEEG signal to better diagnose/treat the newborns. These outcomes are very important to highlight the deficiencies that current electrodes suppose, stating that aCUP-E is a viable alternative.

Through the conducted bibliographic investigation, it has been seen how EEG eclipses a great part of the research, putting less efforts on aEEG. For this reason, it is not a fully developed field, where there is room for improvement. Neonates need a fast diagnosis, in which electrodes play a crucial role. Ensuring low impedance levels as well as its stability are essential.

In this study a code has been developed to create the aEEG signal from raw EEG exported from the CFM. This program can be useful for clinicians and researchers to obtain the aEEG signal and be able to process it in a computer, with expanded capabilities. Still, this tool should be further developed integrating more aspects of interests for researchers, and an easier access for clinicians. Moreover, a standardized procedure is required, where the filters and techniques used to process the raw EEG should not be something with which companies compete.

The proposed neurophysiology criteria have made it possible to achieve the goal of determining optimal and non-optimal brain activity. It has been observed that aCUP-E records larger optimal brain activity compared to the commercial ones, indicating their lower sensitivity to various artifacts. These results show potential to enable clinicians to rapidly diagnose and perform long aEEG recordings.

The hypothesis that the signal obtained from both hemispheres should be very similar was verified in segments in which an optimal brain bioelectric activity was recorded for two consecutive hours. The findings have reinforced the idea that both brain hemispheres develop simultaneously in neonates and rejected that under ideal conditions both electrodes capture a different signal. Moreover, the importance of electrode positioning, which is related with the trace width, was highlighted, showing that along the clinical trial an accurate placing of the electrodes was achieved. Thus, it has been reasonable to make interhemispheric comparisons, and state that the differences observed in the signal are due to the improved characteristics of aCUP-E.

The previous feature made it possible to quantify the signal quality of each electrode type, in which aCUP-E showed better SNR than commercial electrodes. However, differences were not found regarding susceptibility to noise, since this is a characteristic of the sensor material and it is not an innovative feature of aCUP-E (Ag/AgCl plate for both).

The new electrodes (aCUP-E) stood out for their improved adhesion, which has been the main factor causing the previous signal differences. Lower impedance levels and lower variability have been observed compared to commercial electrodes. Also, the gel refilling feature of aCUP-E is a key factor to obtain a longer electrode life.

For central positions, aCUP-E performed better in terms of impedance stability and electrode life. Still, not significant differences are seen in the parietal locations. This may be due to the fact that aCUP-E electrodes have a high body, which makes them more vulnerable to friction forces. Also, the position of the wire exiting vertically from the electrode is convenient for centrals as it reduces the torque by stretching that the commercials experience but may be counterproductive in parietal electrodes since the wire may increase the effect of the contact with the mattress.

It should be noted that these results come from a clinical trial with neonates, in which different conditions for each newborn are included. So, the differences found in which aCUP-E performs better, are actually significant for their introduction into the clinical practice. These results confirm the previous laboratory tests, which were performed by doing long recordings in an aEEG test bench.

Importantly, the NICU staff survey showed that aCUP-E relieves the workload of the NICUs, where up to now the nurses had to be on the lookout for the impedance level of the electrodes to obtain good recordings. Moreover, the aCUP-E adaptations allow for the kangaroo care method which promotes skin-to-skin contact and is widely used in the NICUs to support physiological well-being of premature neonates. For these reasons, the survey showed a clear willingness of the NICUs personnel to use the new device in aEEG recordings.

Thanks to aCUP-E enhanced performance, in the future, NICUs around the world will be able to perform high quality aEEG recordings, allowing neonatologists to diagnose and treat newborns more efficiently.

5.1 Future work

To improve the performance of the aCUP-E electrodes in parietal positions, several solutions for future projects are proposed to lower the torque that drives them useless. Considering that being able to rest the head in neonates is mandatory:

- Try to improve the material of adhesion. This can be a difficult task, since it has already been studied, and can be controversial because it should not harden the task of removal.
- Lower the heigh. Lowering the heigh of the cup would bring the tangential force closer to the center of mass, reducing the torque.
- Increase the diameter of the ring that is touching the skin, bringing the adhesion force farther and hence increasing the adhesion.

There are different conditions that can produce epilepsy simulations, leading to misinterpretations of the aEEG by the clinicians. Understanding the causes and building a robust aEEG seizure detection algorithm that is able to detect real epilepsy and check if it is not an artifact, would help clinicians to better interpret the traces which is one of the main concerns.

Moreover, assessing the specificity and sensibility of the aCUP-E electrodes could be useful to see whether some specific patterns are better detected, as well as to assess the effect of electrode positioning. For this reason, the sleep-wake cycles could be detected with an algorithm and validated thorough clinical experts. Then we could reconstruct if they allow a better detection by means of a statistical test.

Finally, the created aEEG visualization to display the signal on a computer could add additional features of interest, such as the seizure detection/rejection algorithm and implement it as a *MATLAB Toolbox*, to enable researchers to construct the aEEG signals from the raw EEG. This would allow research to be carried out from studies in which only neonatal EEG was performed, breaking barriers, and helping researchers to investigate in aEEG.

6 Bibliography

[1] I. Benavente-Fernández, S. P. Lubián-López, and A. M. Lechuga-Sancho, "Estudio del electroencefalograma integrado por amplitud normal y patológico, y su relación con el pronóstico, en recién nacidos prematuros de muy bajo peso al nacimiento.," Tesis doctoral, Universidad de Cádiz, Cadiz, 2015. doi: 10.1007/s00431-014-2360-0.

[2] Handryastuti S, "An overview of an amplitude integrated EEG," 2007.

[3] H. C. Glass *et al.*, "Neurocritical Care for Neonates," *Neurocrit Care*, vol. 12, no. 3, pp. 421–429, Jun. 2010, doi: 10.1007/s12028-009-9324-7.

[4] S. W. Foreman, L. Thorngate, R. L. Burr, and K. A. Thomas, "Electrode Challenges in Amplitude-Integrated Electroencephalography (aEEG): Research Application of a Novel Noninvasive Measure of Brain Function in Preterm Infants," *Biol Res Nurs*, vol. 13, no. 3, pp. 251–259, Jul. 2011, doi: 10.1177/1099800411403468.

[5] Z. Wang *et al.*, "Electroencephalography monitoring in the neonatal intensive care unit: a Chinese perspective," *Transl Pediatr*, vol. 10, no. 3, pp. 552–559, Mar. 2021, doi: 10.21037/TP-20-340.

[6] "Brain Anatomy and How the Brain Works | Johns Hopkins Medicine." https://www.hopkinsmedicine.org/health/conditions-and-diseases/anatomy-of-the-brain (accessed Apr. 17, 2023).

[7] "Brain Basics: Know Your Brain | National Institute of Neurological Disorders and Stroke." https://www.ninds.nih.gov/health-information/public-education/brain-basics/brain-basics-know-your-brain (accessed Apr. 17, 2023).

[8] R. Dimitrova *et al.*, "Preterm birth alters the development of cortical microstructure and morphology at term-equivalent age," *Neuroimage*, vol. 243, Nov. 2021, doi: 10.1016/j.neuroimage.2021.118488.

[9] B. A. Brody, C. Kinney, A. S. Kloman, and F. H. Gilles, "Sequence of Central Nervous System Myelination in Human Infancy. I. An Autopsy Study of Myelination," 1987. [Online]. Available: http://jnen.oxfordjournals.org/

[10] J. Kolasinski *et al.*, "Radial and tangential neuronal migration pathways in the human fetal brain: Anatomically distinct patterns of diffusion MRI coherence," *Neuroimage*, vol. 79, pp. 412–422, Oct. 2013, doi: 10.1016/j.neuroimage.2013.04.125.

[11] Y. Zhang, J. Shi, H. Wei, V. Han, W. Z. Zhu, and C. Liu, "Neonate and infant brain development from birth to 2 years assessed using MRI-based quantitative susceptibility mapping," *Neuroimage*, vol. 185, pp. 349–360, Jan. 2019, doi: 10.1016/j.neuroimage.2018.10.031.

[12] M. B. Belfort, "Human Milk and Preterm Infant Brain Development," *Breastfeeding Medicine*, vol. 13, no. S1, pp. S23–S25, Apr. 2018, doi: 10.1089/bfm.2018.29079.mbb.

[13] R. O. Lloyd, J. M. O'Toole, V. Livingstone, P. M. Filan, and G. B. Boylan, "Can EEG accurately predict 2-year neurodevelopmental outcome for preterm infants?," *Arch Dis Child Fetal Neonatal Ed*, vol. 106, no. 5, pp. 535–541, Sep. 2021, doi: 10.1136/archdischild-2020-319825.

[14] H. J. Niemarkt *et al.*, "Multi-channel amplitude-integrated EEG characteristics in preterm infants with a normal neurodevelopment at two years of corrected age," *Early*

Hum Dev, vol. 88, no. 4, pp. 209–216, Apr. 2012, doi: 10.1016/j.earlhumdev.2011.08.008.

[15] V. Jurcak, D. Tsuzuki, and I. Dan, "10/20, 10/10, and 10/5 systems revisited: Their validity as relative head-surface-based positioning systems," *Neuroimage*, vol. 34, no. 4, pp. 1600–1611, Feb. 2007, doi: 10.1016/j.neuroimage.2006.09.024.

[16] M. Seeck *et al.*, "The standardized EEG electrode array of the IFCN," *Clinical Neurophysiology*, vol. 128, no. 10. Elsevier Ireland Ltd, pp. 2070–2077, Oct. 01, 2017. doi: 10.1016/j.clinph.2017.06.254.

[17] B. J. Lipsett, V. Reddy, and K. Steanson, *Anatomy, Head and Neck: Fontanelles*. 2023.

[18] L. Hellström-Westas and I. Rosén, "Continuous brain-function monitoring: State of the art in clinical practice," *Semin Fetal Neonatal Med*, vol. 11, no. 6, pp. 503–511, Dec. 2006, doi: 10.1016/j.siny.2006.07.011.

[19] D. Maynard, P. F. Prior, and D. F. Scott, "Device for continuous monitoring of cerebral activity in resuscitated patients.," *BMJ*, vol. 4, no. 5682, pp. 545–546, 1969, doi: 10.1136/bmj.4.5682.545-a.

[20] R. Dilena *et al.*, "Consensus protocol for EEG and amplitude-integrated EEG assessment and monitoring in neonates," *Clinical Neurophysiology*, vol. 132, no. 4. Elsevier Ireland Ltd, pp. 886–903, Apr. 01, 2021. doi: 10.1016/j.clinph.2021.01.012.

[21] P. F. Prior *et al.*, "Monitoring Cerebral Function: Clinical Experience with New Device for Continuous Recording of Electrical Activity of Brain," *BMJ*, vol. 2, no. 5764, pp. 736–738, 1971, doi: 10.1136/bmj.2.5764.736.

[22] I. Bjerre, L. Hellström-Westas, I. Rosén, and S. NW, "Monitoring cerebral function after severe asphyxia in infancy," *Arch Dis Child*, vol. 58, pp. 997–1002, Apr. 1984, doi: 10.1136/adc.58.12.997.

[23] N. Al Naqeeb, ; A David Edwards, F. M. Cowan, and D. Azzopardi, "Assessment of Neonatal Encephalopathy by Amplitude-integrated Electroencephalography," 1999. [Online]. Available: http://pediatrics.aappublications.org/

[24] R. Del Río, C. Ochoa, A. Alarcon, J. Arnáez, D. Blanco, and A. García-Alix, "Amplitude integrated electroencephalogram as a prognostic tool in neonates with hypoxic-ischemic encephalopathy: A systematic review," *PLoS One*, vol. 11, no. 11, Nov. 2016, doi: 10.1371/journal.pone.0165744.

[25] S. Ouwehand *et al.*, "Predictors of Outcomes in Hypoxic-Ischemic Encephalopathy following Hypothermia: A Meta-Analysis," *Neonatology*, vol. 117, no. 4. S. Karger AG, pp. 411–427, Dec. 01, 2020. doi: 10.1159/000505519.

[26] A. Rakshasbhuvankar, S. Paul, L. Nagarajan, S. Ghosh, and S. Rao, "Amplitude-integrated EEG for detection of neonatal seizures: A systematic review," *Seizure*, vol. 33. W.B. Saunders Ltd, pp. 90–98, 2015. doi: 10.1016/j.seizure.2015.09.014.

[27] G. B. Boylan, N. J. Stevenson, and S. Vanhatalo, "Monitoring neonatal seizures," *Seminars in Fetal and Neonatal Medicine*, vol. 18, no. 4. pp. 202–208, Aug. 2013. doi: 10.1016/j.siny.2013.04.004.

[28] M. Cordeiro, H. Peinado, M. T. Montes, and E. Valverde, "Evaluation of the suitability and clinical applicability of different electrodes for aEEG/cEEG monitoring in the extremely premature infant," *An Pediatr (Engl Ed)*, vol. 95, no. 6, pp. 423–430, Dec. 2021, doi: 10.1016/j.anpedi.2020.09.009.

[29] C. Chen *et al.*, "A digitized approach for amplitude-integrated electroencephalogram transformation towards a standardized procedure," *Biomed Signal Process Control*, vol. 66, Apr. 2021, doi: 10.1016/j.bspc.2021.102433.

[30] D. Zhang and H. Ding, "Calculation of compact amplitude-integrated EEG tracing and upper and lower margins using raw EEG data," *Health N Hav*, vol. 05, no. 05, pp. 885–891, 2013, doi: 10.4236/health.2013.55116.

[31] J. Guerreiro *et al.*, "INSTITUTO SUPERIOR DE ENGENHARIA DE LISBOA A Biosignal Embedded System for Physiological Computing Vowels," 2013.

[32] M. A. Lopez-Gordo, D. Sanchez Morillo, and F. Pelayo Valle, "Dry EEG electrodes," *Sensors (Switzerland)*, vol. 14, no. 7. MDPI AG, pp. 12847–12870, Jul. 18, 2014. doi: 10.3390/s140712847.

[33] N. M. El Ters, A. M. Mathur, S. Jain, Z. A. Vesoulis, and J. M. Zempel, "Long term electroencephalography in preterm neonates: Safety and quality of electrode types," *Clinical Neurophysiology*, vol. 129, no. 7, pp. 1366–1371, Jul. 2018, doi: 10.1016/j.clinph.2018.02.129.

[34] T. Werther, M. Olischar, G. Naulaers, P. Deindl, K. Klebermass-Schrehof, and N. Stevenson, "Are All Amplitude-Integrated Electroencephalogram Systems Equal?," *Neonatology*, vol. 112, no. 4, pp. 394–401, Nov. 2017, doi: 10.1159/000480008.

[35] M. Quigg and D. Leiner, "Engineering Aspects of the Quantified Amplitude-Integrated Electroencephalogram in Neonatal Cerebral Monitoring," 2009.

[36] Z. A. Vesoulis, P. G. Gamble, S. Jain, N. M. El Ters, S. M. Liao, and A. M. Mathur, "WU-NEAT: A clinically validated, open-source MATLAB toolbox for limited-channel neonatal EEG analysis," *Comput Methods Programs Biomed*, p. 105716, Aug. 2020, doi: 10.1016/j.cmpb.2020.105716.

[37] A. Yeung *et al.*, *Comparison of Foam-Based and Spring-Loaded Dry EEG Electrodes with Wet Electrodes in Resting and Moving Conditions**. 2015. doi: 10.0/Linux-x86_64.

[38] A. Delorme and S. Makeig, "EEGLAB: an open source toolbox for analysis of single-trial EEG dynamics including independent component analysis," *J Neurosci Methods*, vol. 134, no. 1, pp. 9–21, Mar. 2004, doi: 10.1016/j.jneumeth.2003.10.009.

[39] G. L. Li, J. T. Wu, Y. H. Xia, Q. G. He, and H. G. Jin, "Review of semi-dry electrodes for EEG recording," *Journal of Neural Engineering*, vol. 17, no. 5. IOP Publishing Ltd, Oct. 01, 2020. doi: 10.1088/1741-2552/abbd50.

[40] J. W. Y. Kam *et al.*, "Systematic comparison between a wireless EEG system with dry electrodes and a wired EEG system with wet electrodes," *Neuroimage*, vol. 184, pp. 119–129, Jan. 2019, doi: 10.1016/j.neuroimage.2018.09.012.

[41] H. Hinrichs, M. Scholz, A. K. Baum, J. W. Y. Kam, R. T. Knight, and H. J. Heinze, "Comparison between a wireless dry electrode EEG system with a conventional wired wet electrode EEG system for clinical applications," *Sci Rep*, vol. 10, no. 1, Dec. 2020, doi: 10.1038/s41598-020-62154-0.

[42] A. Bravi, A. Longtin, and A. J. Seely, "Review and classification of variability analysis techniques with clinical applications," 2011. [Online]. Available: http://www.biomedical-engineering-online.com/content/10/1/90

[43] A. S. Al-Fahoum and A. A. Al-Fraihat, "Methods of EEG Signal Features Extraction Using Linear Analysis in Frequency and Time-Frequency Domains," *ISRN Neurosci*, vol. 2014, pp. 1–7, Feb. 2014, doi: 10.1155/2014/730218.

[44] S. Leske and S. S. Dalal, "Reducing power line noise in EEG and MEG data via spectrum interpolation," *Neuroimage*, vol. 189, pp. 763–776, Apr. 2019, doi: 10.1016/j.neuroimage.2019.01.026.

[45] P. Rebasa, "Conceptos básicos del análisis de supervivencia".

[46] "The notion of Censoring in Survival Analysis | JiGSO." https://jigso.com/the-notion-of-censoring-in-survival-analysis/ (accessed Jun. 09, 2023).

[47] T. Radüntz, "Signal quality evaluation of emerging EEG devices," *Front Physiol*, vol. 9, no. FEB, Feb. 2018, doi: 10.3389/fphys.2018.00098.

[48] S. E. Lapinsky and A. C. Easty, "Electromagnetic interference in critical care," *J Crit Care*, vol. 21, no. 3, pp. 267–270, Sep. 2006, doi: 10.1016/j.jcrc.2006.03.010.

[49] M. S. Lee, A. Paul, Y. Xu, W. D. Hairston, and G. Cauwenberghs, "Characterization of Ag/AgCl Dry Electrodes for Wearable Electrophysiological Sensing," *Frontiers in Electronics*, vol. 2, Jan. 2022, doi: 10.3389/felec.2021.700363.

Annex

Annex 1 – NICU Staff Survey

Name of the clinical research	
CRD version number	CRD_aCUP-E_v1
Research Centre	Hospital Universitari Sant Joan de Reus
Subject identification number	#
CRD number or date of consultation or consultation number	001
Date of inclusion	DD/MM/AA

Variable de estudio		Metodología	Standard	aCUP-E
Ease of electrode placement and removal	Indicates ease of electrode placement	Likert scale: Very much: 4 Quite a lot: 3 A little: 2 Not at all: 1		
	Indicates the comfort of handling the baby with the electrode	Likert scale: Very much: 4 Quite a lot: 3 A little: 2 Not at all: 1		
	Indicates ease of electrode removal	Likert scale: Very much: 4 Quite a lot: 3 A little: 2 Not at all: 1		
Skin safety	The scalp should be examined at least twice a day to evaluate the presence of skin irritation. The NSCS (Neonatal Skin Condition Score) scale should be used.	Dryness 1 = Normal, no signs of dry skin 2 = Dry skin, visible flaking 3 = Very dry skin, cracking or fissures		
		Erythema 1 = No erythema 2 = Visible erythema <50% of skin surface area 3 = Visible erythema ≥50% of skin surface area		
		Breakage/deterioration of the skin 1= No breakage 2= Small, in localized areas 3= Extensive		
		Perfect score: 3 Worst score: 9 **Total score**		
NOTES				

In the notes section, any data to be collected that the clinical staff identifies and considers to be of special relevance should be added. On the other hand, any extra documentation that is considered appropriate can be added, as well as additional aspects.

Annex 2 – aEEG reconstruction filter

For the same segment (case 1 commercials), different examples of aEEG fitting with filters of different orders. This segment has been chosen because it has decent as well as bad (detached) signal capture. Also, the asymmetric filter is shown where the attenuation of the frequencies changes with different orders.

- Order 300: Does not follow the aEEG model when not properly recording.

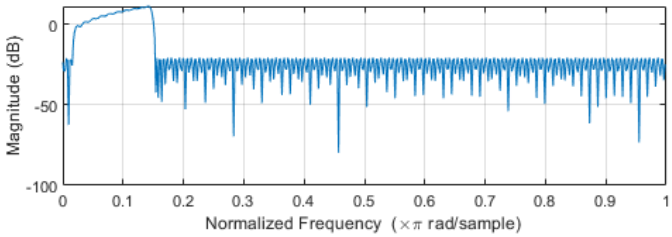

- Order 900: Performs better than the previous one but fails when following the aEEG model when not properly recording.

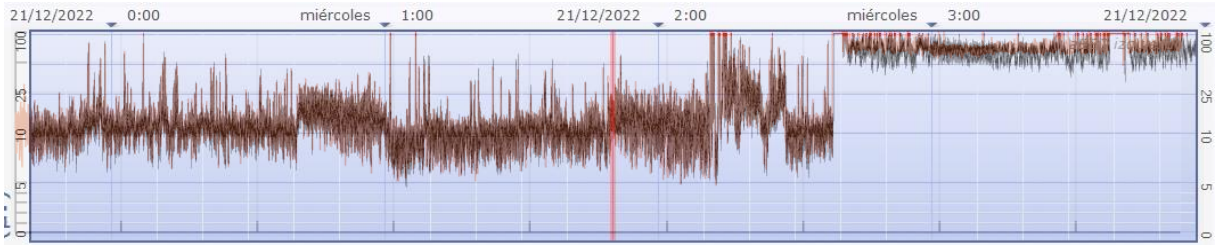

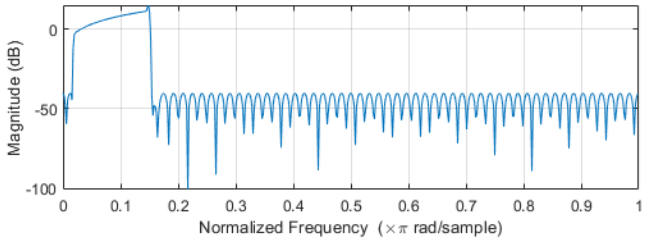

- Order 1100 (Optimal fit): Follows the aEEG in both states, good and bad signal capture.

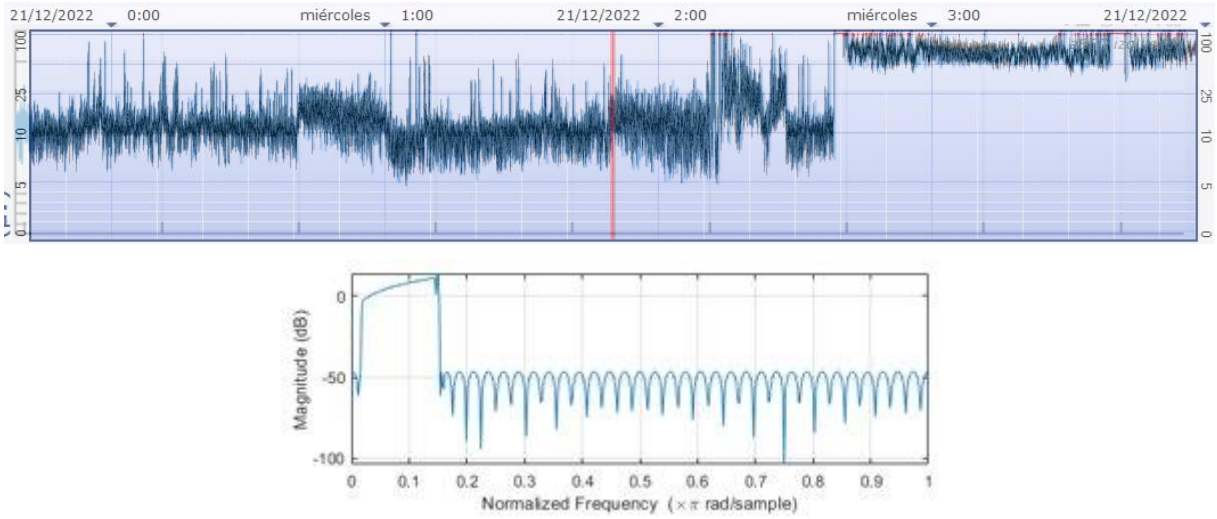

- Order 1200: It works well, but the longer processing time do not compensate for the little improvements in signal reconstruction.

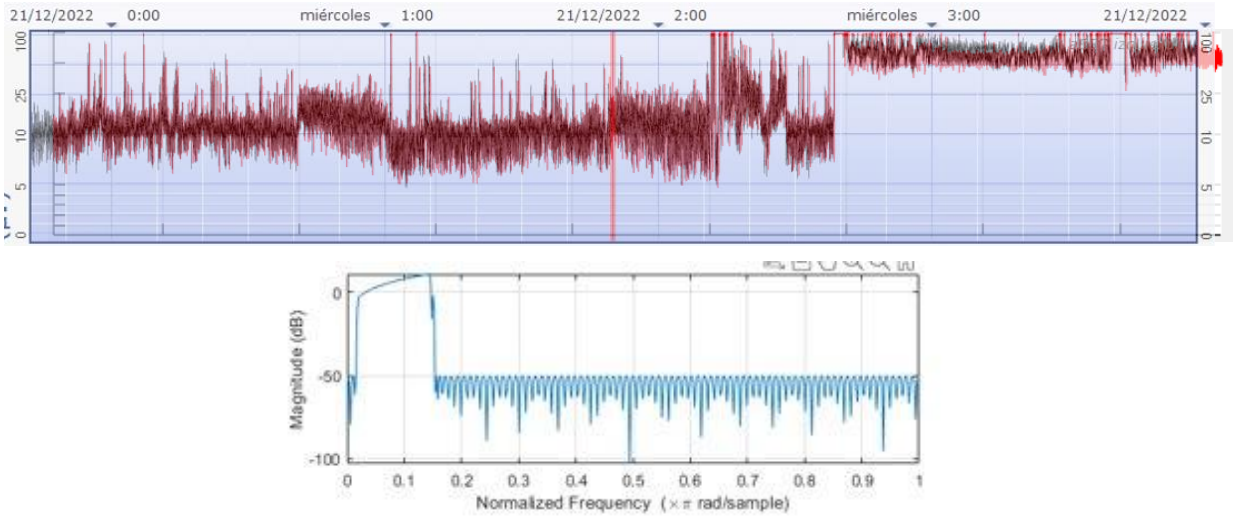

- Order 1300: Also follows the aEEG, but the computation time was too long for the little improvements regarding order 1100.

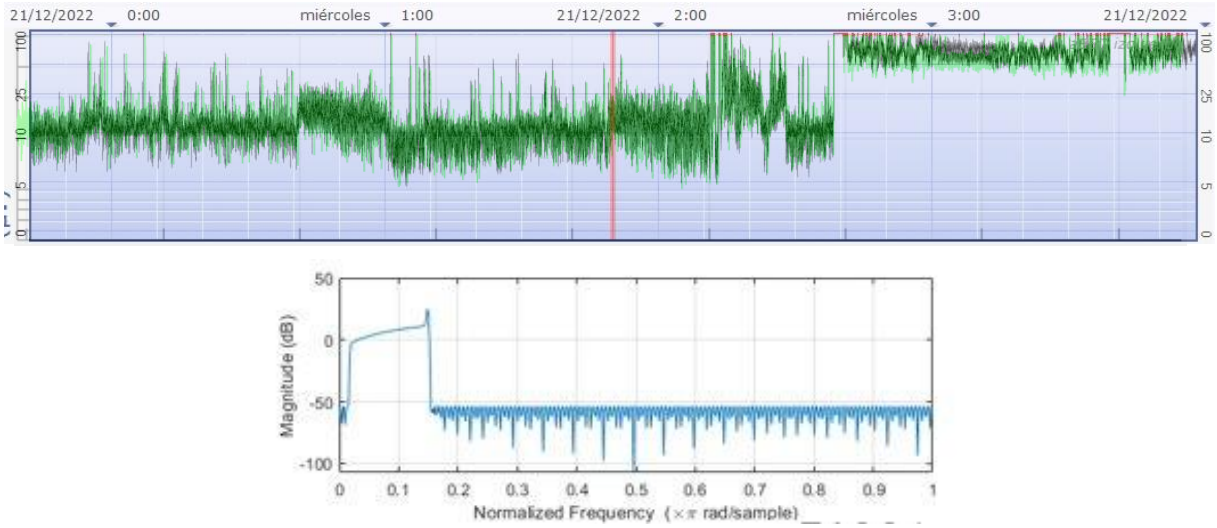

- Order 1400: Very similar to 1300, but more computation time to perform the filtering of the signal.

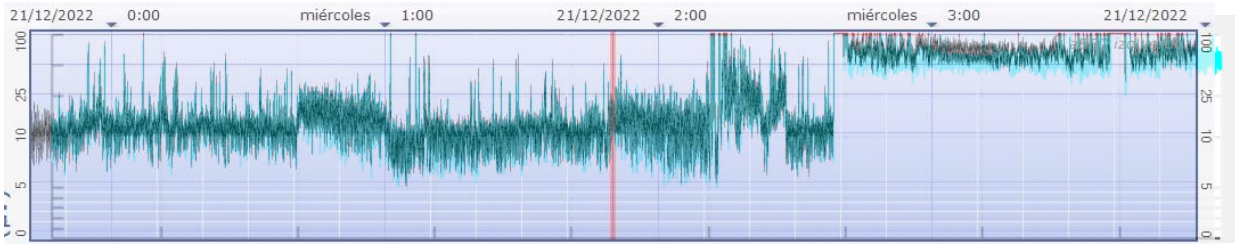

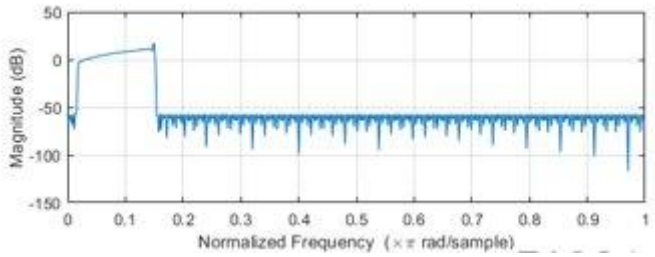

Annex 3 – Source Code

GitHub repository: https://github.com/anrodriba/TFG. Private access.

- *create_aEEG.m:* Code with the functions to build the aEEG and the interface from the raw EEG. The data has to be previously extracted from the CFM and converted to CSV.
- *ParameterFunctions.m:* Code with the functions to get the main parameters from the signals (impedance curves, raw EEG and created aEEG).
- *Results_code.mlx:* Code to see how the data obtained with the functions in *ParameterFunctions.m* was used to generate graphs and obtain the statistics.